

The deep crustal magnetic structure of Britain

David Beamish, Geoff Kimbell and Tim Pharaoh

British Geological Survey, Keyworth, Nottingham, NG12 5GG, UK.

dbe@bgs.ac.uk, gsk@bgs.ac.uk tcp@bgs.ac.uk

Proceedings of the Geologists' Association 127 (2016) 647–663

<http://dx.doi.org/10.1016/j.pgeola.2016.10.007>

Corresponding author:

David Beamish

British Geological Survey, Keyworth, Nottingham, NG12 5GG, UK

Email: dbe@bgs.ac.uk

Tel: +44(0)115 936 3432

Fax: +44(0)115 936 3437

Keywords: Magnetic anomalies, modelling and interpretation, rock and mineral magnetisation, subduction zone, tectonics.

ABSTRACT

The deep crustal magnetic structure of Britain has not previously been described in a uniform manner. We provide a new assessment of the deep crustal magnetic bodies responsible for the long wavelength magnetic features. The study area contains deep crustal relics of the destruction of early Palaeozoic oceanic lithosphere along the Thor-Tornquist Suture and primarily the Iapetus Suture separating Baltica and Avalonia from the Laurentian terranes. Spectral decomposition is applied to a merged onshore and offshore magnetic anomaly data set. Thirty idealised basement bodies are compared with a representation of the subsurface obtained by a coarse 3D inversion of the data. The central area separating Laurentia and Avalonia, is largely characterised by an absence of high susceptibilities throughout the whole crustal volume. We find that the idealised basement bodies are largely consistent with relatively high susceptibility zones at depths in excess of 10 km. The zones of higher relative susceptibility are referenced to the tectonic-terrane framework of the area and possible geological explanations for the contrasts are reviewed. In the north, the Laurentian terranes are diverse, comprising crust first created in the Archaean (Hebridean Terrane), Palaeoproterozoic (Rhinn's Terrane), Mesoproterozoic? (Midland Valley Terrane), Neoproterozoic (sub-Southern Upland rocks) and Ordovician. Magnetic anomalies further record the assembly of the Gondwanan (Eastern Avalonian) part of the country through Neoproterozoic and Ordovician (Tornquist) arc magmatism and accretion. The convergence zones between Laurentia, Avalonia and Baltica have all left a magnetic imprint, as has Variscan convergence to the south.

1. INTRODUCTION

The tectonic framework of Britain and Ireland was presented in the map produced by Pharaoh *et al.* (1996). The map defines recognised major structures, divisions and sub-divisions at the crustal scale. Here we use as a reference the 15 terranes and 2 sub-terranes shown across the study area (700 x 1250 km) in Figure 1. Table 1 provides details of the codes used. The study area, defined by available airborne and marine magnetic survey data, sits within the wider tectonic framework of western Europe. This more extensive setting is discussed by Pharaoh (1999) and more recently by Lyngsie *et*

al. (2006). The most significant terrane boundaries are those associated with destruction of early Palaeozoic oceanic lithosphere such as the Thor-Tornquist Suture separating Baltica and Avalonia and the Iapetus Suture separating Baltica and Avalonia, from the Laurentian terranes to the NW. The triple junction between these three Ordovician palaeocontinents is inferred to lie beneath the North Sea, to the east of the study area (e.g. Soper *et al.* 1992; Lyngsie *et al.* 2006). Within the study area, the Laurentian and Avalonian terranes are separated by the Iapetus Suture Zone (Soper *et al.* 1992), which is concealed beneath the Carboniferous Solway-Northumberland Basin and inferred to dip northwards beneath the Southern Upland Terrane (SUT, Fig. 1). Accretion of Avalonia and related terranes was completed in early Palaeozoic time. The orogenic Variscan Front (the northern margin of the Variscide Rhenohercynian Zone or VRZ) represents a later displacement superimposed on the original accretionary mosaic.

TABLE 1

The main method of characterising the magnetic character of the deep crust across Britain has traditionally been through 2.5D profile modelling. The modelling has typically used both magnetic and gravity anomaly variations alongside structural information provided by outcrop mapping and (where available) results from boreholes and seismic surveys. The joint modelling of magnetic and gravity variations is then further controlled by judgements of the geological-tectonic (i.e. 'terrane') framework along the profile. This understanding guides the geometries of the polygons of juxtaposed geophysical properties. The framework is required to reduce inherent ambiguities of non-uniqueness. These methods have been widely applied to the UK aeromagnetic and land-based gravity data within 3 large and overlapping regional areas of South East England, Southern Scotland & Northern England and Northern Scotland (Busby *et al.* 2006; Kimbell *et al.* 2006; Rollin, 2009, respectively). Further examples are provided by Trewin & Rollin (2002) who summarise crustal-scale geophysical models across Scotland.

An example of existing combined magnetic and gravity profile modelling across the Hebridean area (identified in Figure 1 and traversing 3 terranes) is shown in Figure 2. The Outer Hebrides (the island chain in the west) is dominated by Archaean and Proterozoic gneisses (Lewisian) which are of comparable age to rocks forming the Caledonian foreland to the east. The two are separated by a sediment filled Mesozoic basin (the Minch). The Outer Isles Thrust (OIT), or fault zone, indicated in Figure 2, has been active since the Proterozoic. Goodenough *et al.* (2013) discuss shear zones and the ages of possible terrane accretion events across the area. Figure 2a shows the existing magnetic data across a rectangular area defined by a 200 km profile discussed below. The image uses a histogram-equalised colour range from 1045 nT (bright red) to -1054 nT (dark blue).

The 2.5D crustal-scale profile model shown in Figure 2b is taken from the regional geophysical guide of Northern Scotland (Rollin 2009). In that study a large number of profiles of both magnetic and gravity data have been used to derive crustal-scale models of the joint distribution of susceptibility and density. Profile 5 (Fortrose) extends into the Hebridean area as the line A-B (Fig. 2a,b) and continues further to the SE beyond the Great Glen Fault (GGF) to provide a profile length of about 200 km. Only the upper 8 km of the cross-section is shown since the basement susceptibilities indicated are uniform to lower crustal depths. The observed and modelled magnetic data along the profile are shown in the upper section of Figure 2b. Some of the modelled deviations are necessarily

caused by the requirement to jointly fit the observed gravity data using density variations within the same set of constructed polygons.

The highest wavenumber contributions in the magnetic data derive from near-surface structures in the footwalls of the Outer Isles Thrust (OIT) and the Moine Thrust Zone (MTZ) on the mainland. These features appear in the model as zones of increased basement susceptibilities which are required to model the long wavelength magnetic behaviour. The western-most zone, associated with Lewisian basement in the vicinity of the OIT, has locally high values of 0.018-0.020 SI while the mainland area in the vicinity of the MTZ is associated with much higher values of 0.040 SI. All the anomalies in the model are generated by a combination of variations in the depth to the magnetic basement and lateral variations in the basement susceptibilities. The depths to magnetic basement along the profile range from zero (at-surface) to about 6 km.

The purpose of the present study is to provide an extended *mapping* investigation of the deepest magnetic contrasts within the crust and their associations with tectonic terranes. Magnetic modelling is inherently ambiguous and requires guidance and informed constraints to arrive at a plausible understanding of the observations. Ambiguity in depth resolution is particularly problematic. The deep crustal magnetic structure of the study area has not been previously assessed in a uniform manner. In order to provide this assessment we use the compilation of aeromagnetic and marine magnetic data sampled as shown in Figure 3a and the derived magnetic anomaly field grid (500 m cell size) shown in Figure 3b. It is evident that magnetic anomalies exist at all scales and across all terranes. One of the standard issues associated with assessments of such data is the wide and highly variable superposition of the differing wavelength and amplitude contributions associated with shallow and deeper sources. Here we refer to 'sources' as regions associated with higher susceptibilities. Equally the regions between 'sources' are associated with lower susceptibilities. In order to simplify the assessment of deep (basement) magnetic sources we use a technique referred to as matched band-pass spectral filtering. In the simplest case, it may be assumed that the observed field is the sum of the regional (basement) field, a residual (shallow) field and a noise component. The more general model takes into account the shape of the observed spectrum and allows for a general multi-layer case. The derived lower half-space data is compared with more conventional filtering operations including upward continuation.

The constraints on the depth extent of deep magnetic sources have been discussed by Kimbell and Stone (1995). On the basis of xenolith samples, Wasilweski *et al.* (1979) and Wasilewski & Mayhew (1992) concluded that the Moho typically forms a magnetic boundary, with magnetic minerals being largely absent in the upper mantle. This interpretation has been questioned by Ferré *et al.* (2013, 2014), who identified ferromagnetic minerals (most commonly magnetite) in mantle xenoliths, although their measured magnetizations would only produce small contrasts of around 0.02 to 0.03 A/m (Ferré *et al.* 2013), which is equivalent to susceptibility contrasts of less than 0.001 SI. For comparison, modelling of mid-crustal magnetic sources responsible for long-wavelength magnetic anomalies over Britain typically requires magnetisations equivalent to susceptibilities of 0.02 to 0.04 SI (Kimbell & Stone 1995; Kimbell & Quirk 1999). Highly magnetic zones could occur within the upper mantle as the result of its hydration to serpentinite. For example, Blakely *et al.* (2005) correlated long wavelength magnetic anomalies over the Cascadia convergent margin with a wedge of serpentinitized mantle above the subduction zone and below the Curie temperature for magnetite (c. 580°C). In Britain with a typical crustal thickness of about 30 km and heat flow of 50-60 mW/m³, the

uppermost part of the mantle may lie below the Curie temperature. However, the tops of the magnetic blocks identified by the present study all lie within the crust, and these blocks are unlikely to be continuous with serpentinized upper mantle at depth, so it is considered reasonable to regard the Moho as the limit for their bases. For this study we have made the assumption that the major deep sources of magnetic anomalies beneath the UK are typically magnetised in the direction of the Earth's present magnetic field. This is on the basis of the tendency for long-lived remanent magnetisations to cancel each other out in large and complex rock volumes and because of the increasing importance of short-lived viscous remanent magnetisation at greater depths (Kimbell & Stone 1995).

A wide range of magnetic source-edge detection methods have been developed to assess 'idealised' body edges, their depths and possible geometrical (structural) signatures. Generally, using these simplified methods, the spatial location (edges) of the assumed simple-geometry sources is more accurate than secondary parameters such as depth, dip, strike and structural index (e.g. Nabighian et al., 2005). The magnetic anomaly data used for this study (Fig. 3a) are of variable quality and the derived grid is subject to variable interpolation. This suggests a requirement to use only techniques which employ first-order spatial derivatives rather than higher-order terms which introduce additional noise. Although we have considered a wide-range of approximate grid-based procedures, we use the tilt-derivative (Millar and Singh, 1994) for locating contact edges.

The analyses undertaken delineate a series of deep, positively magnetised zones across the study area. We refer to these as idealised basement bodies. In order to confirm and refine the definition of the idealised bodies and their associated depths we carry out a largely unconstrained, 3D inversion of the data set. Although the comparison of the 2D plan view bodies and the continuous 3D distribution of susceptibility values is not simple, the assessment allows the majority of the basement anomalies to be identified as deep (e.g. ≥ 10 km) sources.

The basement bodies, associated with areas of higher relative susceptibility, provide a useful summary map and are referenced to the tectonic-terrane framework discussed above. The identified sources of the long-wavelength magnetic anomalies over Laurentian (northern) and Eastern Avalonian (southern) Britain inevitably reflect the detail of complex processes involved across the early Palaeozoic convergence zones between the Ordovician palaeocontinents of Laurentia, Avalonia and Baltica.

2 MATERIALS AND METHODS

2.1 Data

The baseline aeromagnetic data for the UK (largely onshore) were acquired between 1955 and 1965. The flying height was about 305 m and flight line spacing was typically 2 km (Beamish & White, 2011). The aeromagnetic data have been merged with (i) a compilation of existing marine survey magnetic data sets (North Sea, English Channel and SW Approaches) and (ii) existing data from eastern Ireland to provide a largely consistent and comprehensive magnetic anomaly data set covering latitudes from 49.7° to 61.1° and longitudes from -9.4° to 3.0°. This defines a survey extent of 700 x 1250 km as shown in Figure 3a. A 1:1.5M map of the majority of the data is given in British

Geological Survey (1998). The merged data set comprises 1,223,792 data points. The data are shown in Figure 3b using an equal-area colour image. The data shown are Total Magnetic Intensity (TMI) anomalies, reduced-to-pole (TMI-RTP).

As indicated in Figure 3a, the spatial sampling of the merged data is variable particularly in the vicinity of the edges of the higher resolution UK aeromagnetic surveys. The typical maximum grid resolution (using a quarter-wavelength sampling criterion) that can be justified using the baseline data is 500 x 500 m. This grid parametrisation was applied to the merged data set using a minimum curvature algorithm with interpolation through data gaps. The interpolation procedure produces some artefacts in the high wavenumber components of the data but is adequate for the longer wavelength components considered here. Two zones with no data coverage, in the NE and SE corners of the study area are omitted from the analysis.

The shape of magnetic anomalies varies as a function of geomagnetic latitude. For UK data, it is useful to transform the data using reduction-to-pole or RTP (Blakely 1995), generating anomalies that peak over the source location. The analyses conducted are based on RTP transformed magnetic anomaly data. Some igneous units and cultural noise sources may provide anomalies with remanent magnetisation directions that violate the assumption. Structures providing normally and reversely magnetised fields should be adequately represented in terms of their source location.

2.2 Processing Techniques

Spatial derivatives have a well-established role in the interpretation of potential field data from magnetic surveys. There exists a range of processing procedures and filters, largely relating to vertical and horizontal derivatives and their combinations that perform as enhanced mapping functions when applied to the basic data sets (Blakely 1995; Li 2003). Here we consider methods developed for gridded magnetic data sets.

In the approximate methods discussed here, the structural index (i.e. the geometrical form of the body) has to be considered either implicitly or explicitly (Reid & Thurston 2014) particularly when estimating secondary parameters such as depth. The plethora of methods that have been developed to estimate both primary and secondary body parameters may be considered to be attributable to the (i) the nature of the underlying assumptions, (ii) the noise level of the different data sets. To obtain an estimate of the over highly magnetic bodies associated with the long-wavelength (basement) field we here use the tilt-derivative (TDR) (Miller & Singh 1994) to obtain estimates of body edge locations. Prior to the application of such procedures, the data are spectrally decomposed to isolate the deep(est) component of the magnetic field response, as discussed in the next section. The intention is to provide a summary of the deepest magnetic contrasts within the crust and their associations with tectonic terranes.

The edge-detection procedure is applied to the longest wavelength features of the data set, across all sources, and is approximate. The associated depth-estimation procedures currently in use (Salem et al., 2005, 2007) typically assume that the idealised bodies are spatially isolated and locally 2-dimensional and that the contact has an infinite depth extent. The former assumption may have limited applicability in relation to deeper basement sources as may be judged from the example cross-sectional model of Figure 2b. Flanagan and Bain (2013) also note depth errors as high as 40% when the assumption of infinite depth extent is made. When considering assessments of mid- to

deep-crustal sources, the practical depth extent of potential sources is also restricted by the (assumed) limit of 30 km. In order to evaluate the idealised edge-detection mapping results, they are compared with a volumetric crustal-scale 3D inversion model of the complete data set. This allows both the magnitudes and the depth distribution of the idealised sources to be assessed.

2.2.1 Matched band-pass spectral filters

In order to examine the longer wavelength components in the data we use a technique referred to as matched band-pass spectral filtering that extends the original procedures described by Spector & Grant (1970) and Syberg (1972). Here we follow the procedures described by Phillips (2001). The general model takes into account the shape of the observed spectrum and allows for a general multilayer case and considers the effects of sources at a number of distinct spectral/depth levels. The physical significance of the number of layers and their thicknesses remains questionable given the equivalence inherent in such a modelling procedure (Pedersen 1991).

Using a graphical procedure, the plot of the logarithm of energy against wavenumber is used to establish a number of straight-line segments (a matched filter model) whose slopes are then optimised to minimise the residual spectrum between that observed and that calculated from the model layers. The layered model terminates in a magnetic half-space that provides a linear spectrum at all wavenumbers. The half-space estimate is effectively formed by a low-pass filtering operation. Here we assume that this half-space forms an estimate of magnetic basement. This optimised half-space magnetic data set forms the basis of the magnetic basement structural model considered here. The depths obtained by the analysis are treated as approximate and the procedure is essentially used to obtain the distribution of magnetic source bodies responsible for the longest wavelengths.

2.2.2 Upward Continuation filters

The procedure of upward continuation is a specific form of wavelength filtering and is essentially used to calculate the potential field of a data set at an altitude greater than that of the measured height. In the Fourier domain, upward continuation is achieved by a simple exponential transform (Blakely 1995, equation 12.8) that reduces the high wavenumber content of the data set and also reduces spatial resolution. The procedure operates by Fourier transforming the measured data, multiplying by the exponential transform and then inverse Fourier transforming the product. The transform is a specific form of low-pass filtering operation. The exponential transform is considered a 'clean' form of filtering since it produces almost no side effects. Upward continuation was used as a form of regional/residual separation in the large scale study of Lyngsie *et al.* (2006) and multi-scale (sequential) upward continuations have been used as a means of depth to source estimation (Fedi *et al.* 2012). Here upward continuation is used only as a means of low-pass filtering.

2.2.3 The Tilt Derivative (TDR)

Structural edge information in the data is examined here using the Tilt Derivative (TDR) as described by Miller & Singh (1994). The tilt derivative or tilt angle is defined as the arctangent of the ratio of a vertical to a combined (total) horizontal derivative. The amplitude range is restricted to $\pi/2$ to $-\pi/2$ (or 90° to -90°) by virtue of the arctan function, such that the TDR acts as an Automatic Gain Control (AGC) filter when applied to the observations. The TDR responds *equally* to both shallow and deep sources. When considering the magnetic basement (deep) responses, as here, the TDR is a simplified and highly effective edge mapping function.

Existing modelling of the TDR response to isolated magnetic bodies (e.g. Fairhead *et al.* 2004; Verduzco *et al.* 2004; Cooper & Cowan 2006; Salem *et al.* 2007) indicate that the TDR is positive when over the source, it passes through zero when over (or near) the edge of the source, where the vertical derivative is zero and the horizontal derivative is a maximum, and is negative outside the source region. The sources considered (e.g. basement steps, blocks and dykes) are effectively normally magnetised.

2.2.4 3D magnetic inversion

In order to obtain a more rigorous assessment of the subsurface distribution of magnetic sources we have undertaken 3D inversion of a down-sampled version of the data set shown in Figure 3b. The inversion method used was originally developed by Li and Oldenburg (1996) and is referred to as MAG3D (or UBC-GIF). The algorithm assumes that the measured magnetic field is produced only by induced magnetization and that no remanent magnetization is present. The subsurface distribution is represented by a large number of rectangular cells of constant susceptibility, and the final solution is obtained by finding a model that reproduces the data adequately and at the same time minimizes a model objective function penalizing the structural complexity of the model (the model is inherently smooth). A depth or distance weighting function is applied to counteract the decay of sensitivity with depth. The most informative results are obtained when the model can be constrained by structural, geological or existing information e.g. on the true range of susceptibilities (e.g. Spicer *et al.*, 2011). Such constraints are more difficult to apply when a crustal model on the scale of the present study area is considered. Here, following a series of assessments, we present a 3D susceptibility model that is best described as exploratory rather than definitive.

3 RESULTS

The results discussed here use the TMI-RTP data in grid form at 500 m (e.g. Fig. 3b) and along profile A-A' as shown in Figures 1 and 3b.

3.1 Matched band-pass filtering

The optimisation of the matched band-pass procedure to fit the observed radial spectrum required the definition of 4 layers above an underlying half-space. The spectral depths associated with each layer were 407 m (MAG4), 1609 m (MAG3), 5018 m (MAG2) and 16,630 m (MAG1), as shown in Table 2. The spectral depth of the underlying half-space was estimated as 35,250 m (MAG0). The latter depth is clearly unphysical and we regard it as an artefact. A simple 4-layer model is unlikely to be a valid assumption across the entire study area. The longest wavelength (i.e. > 50 km) contributions to the spectrum are also likely to be influenced by data-merging artefacts (e.g. Fig. 3). The spectral depths obtained are therefore not used; we only use the matched-filtering procedure to obtain an estimate of the deep-crustal field. For interpretation we only use this filter to obtain the geometries (not depth) of the deep bodies. The matched-filter estimates are compared with the geometries obtained by a range of different filters and found to be equivalent.

Spectral decomposition was accomplished using Wiener band-pass filters to provide the magnetic variations associated with each layer. The initial near-surface layer apparent depth is close to the grid sampling interval of 500 m and, as expected, largely comprises noise with some leakage from

the underlying layer. The main focus of the analysis is the magnetic response from the underlying half-space (here termed MAG0).

TABLE 2

The results obtained are illustrated in Figure 4 using equal-area colour scaling of the filtered magnetic field variations defined in Table 2. In Figure 4a, MAG3 contains some residual sampling noise when examined in detail. The image sequence shows the expected progressive behaviour of increasing wavelength with increasing spectral depth. Figures 4a and 4b (MAG3 and MAG2) summarise the main character of near-surface magnetic variations. The intense localisation of features in northern Britain (north of the Southern Upland Terrane, SUT) is very evident as is the response of the Antrim lavas of Northern Ireland. Figure 4b (MAG2) shows more evidence of the lower amplitude magnetic fabric particularly within Avalonia (south of the SUT). It is likely that MAG1 (Fig. 4c) represents a wavelength transition between the shallow magnetic features and the basement magnetic response represented in Figure 4d by MAG0. The basement magnetic response observed indicates a series of magnetic bodies across Laurentia (to the north of the SUT) and a series of bodies within the core of Avalonia, with a clear boundary (anomaly edge) formed by the Variscan Front (VF).

3.2 Low-pass filter comparisons

3.2.1 Along profile

A comparison of the half-space MAG0 response with that obtained using other, alternative, low-pass filter operators was undertaken using the data along profile A-A' shown in Figures 1 and 3b. The profile traverses all the major terranes and is 1328.5 km in length. Figure 5 shows the original TMI-RTP data (with infill) and the MAG0 data (in red) along the profile. The MAG0 response isolates a series of longer-wavelength features defined by 9 major positive excursions and their associated minima. The MAG0 response is compared with two upward-continued filter responses at continuation levels of 10 km and 20 km. Both of these operators provide a more conservative (less peaked) low-pass filtering of the data. Finally a Gaussian regional filter with a standard deviation (equivalent to a filter cut-point) of 60 km is shown. This filter was found to provide a response that is very similar to the MAG0 response.

The ability of the low-pass filtering operators to adequately represent deep-seated basement features is partially a function of the amplitude levels and locations of any short wavelength features encountered. The majority of long wavelength features identified in the MAG0 response (Fig. 5) appear to be representative of the features in the underlying TMI-RTP data. A departure from this occurs in the vicinity of the Moine Thrust Zone (MTZ). Figure 6 shows a more detailed assessment of the TMI-RTP data and the MAG0 response across a profile distance from 200 to 700 km. Generally the MAG0 data provide adequate characterisation of the long wavelength peaks and troughs as can be seen in the case of the isolated anomaly associated with Great Glen Fault (GGF). In the case of the variations to the north of and across the Moine Thrust Zone (MTZ), the extraction of a representative 'basement field' may be unrealistic.

3.2.2 Maps (TDR)

The zero value of the tilt-derivative (TDR) is used here for the edge detection of source bodies. The TDR function gives equal weight to all amplitudes and may therefore amplify noise. The variation of the TDR source edge estimates derived from a subset of the different filters considered above in relation to the profile data are shown for the complete data set in Figure 7. Here the source locations ($TDR \geq 0$) obtained from the MAG0 data are shown with infill. These are then compared with the equivalent edges ($TDR = 0$) obtained by upward-continuation (10 km) and by a Gaussian regional filter (60 km cut-point). It is evident that at the large scale all three data sets provide largely consistent estimates of the deep source bodies. At the more detailed scale, the latter two data sets appear to contribute some additional and shorter wavelength features. Since the filtering parameters connected with the latter two procedures are somewhat arbitrary, the optimised MAG0 response is preferred when assessing the source body edge locations. The bodies identified by this analysis are referred to as the MAG0-TDR response and are defined for $TDR > 0$ as shown in Figure 7.

3.3 Upward-continuation comparisons

It is possible to further isolate long-wavelength components of the data by increasing the level of upward continuation beyond the 20 km limit considered above. We have assessed upward continuation levels from 20 km to 120 km and the resulting fields from 3 of these levels (20 km, 80 km and 120 km) are shown in Figure 8. In Figures 8b and 8c, the $TDR=0$ contour (theoretically outlining a source body) is shown for reference (white dotted line). For upward continuation levels greater than about 60 km, the anomaly pattern stabilises to that shown in Figures 8b and 8c. The results shown in Figures 8b and 8c represent the simplest description of the large-scale extent of positively magnetised zones in the data set and they clearly form a distinct northern (Laurentian) and southern (Avalonian) zonation. Separating the two is the extensive low centred on the Southern Upland and Leinster-Lakesman terranes (SUT and LLT, Figure 1) and encompassing the Iapetus Suture Zone.

Using the $TDR=0$ contours shown in Figure 8c, the southern zonation is simpler to relate to the existing terrane framework. The northern limit of the Avalonian zone partially tracks the southern margin of the Leinster-Lakesman terrane (LLT, Figure 1) before crossing the Variscan Front (VF) and entering the VRZ (Variscide Rhenohercynian Zone, an orogenic overprint) to the south. The eastern limit of the Avalonian body also partially tracks the eastern limit of the CSB (Caledonians of Southern Britain, Fig. 1).

In the north, the central Laurentian anomaly has a western margin within the Highland Terrane (HT, Fig. 1) which then abuts the terrane boundary associated with the MTZ before forming a distinct western limb (labelled L in Fig. 8b). This long-wavelength feature appears associated with the geometrically-acute southern margin of the Hebridean Terrane (HT, Fig. 1). The southern extent of the central Laurentian anomaly has an E-W attitude and obliquely crosses a sequence of terranes before trending northwards to display a partial association with the eastern boundary of the CHGT (Central Highlands Grampian Terrane).

It is worth noting that the images shown in Figure 8 are equal-area histogram normalisations of each data set. With increasing upward continuation distance we increase the source-receiver separation and anomaly amplitudes reduce accordingly. Using the data resolved along the profile B-B' shown in Figure 8, we note that the full range of the original data is 1568 nT. This compares with data ranges of 173 nT (Fig. 8a, 20 km level), 76 nT (Fig. 8b, 80 km level) and 60 nT (Fig. 8c, 120 km level).

3.4 3D inversion

The original TMI (not TMI-RTP) data were upward continued to a height of 1700 m, which, given a survey elevation of 300 m, provides an equivalent sensor elevation of 2 km. The procedure was applied in order to reduce the short wavelength noise which would detract from the inversion assessment. These data were then gridded at a cell-size of 5 km (generating 141 x 251 cells or 35391 observations) in order to provide a practical assessment of gross crustal structure across the study area. An image of the reduced data set is shown in Figure 9a. The model for the core study area was discretised using horizontal cell sizes of 5 km and vertical cell sizes of 2.5 km to a depth of 30 km. The core study area is thus characterised by 420,000 cells. Padding cells are then added to the 3D core volume to allow for the influence of variations beyond the study area. Padding cells in the vertical direction below 30 km are not strictly required in this case. More localised anomaly assessments benefit from much better control using a regional model extending beyond the study area (e.g. Li and Oldenburg 1998, Goodwin et al., 2015).

The construction of an inverse model using MAG3D proceeds using a range of controls, constraints and knowledge of the data errors (the desired misfit between model and observed responses). The latter is particularly significant in order to avoid modelling noise. We have explored a range of inversion models on the basis that there is a high degree of uncertainty in the reference models and constraints that can be applied to this large and crustal scale problem. We present a final model of susceptibilities that displays common behaviour across the range of models investigated. Both depth-weighting and radial-distance weighting (Goodwin et al., 2015) have been considered.

We have adopted a uniform and highly optimistic data error of 2 nT for the data set. We find that bounding the model susceptibilities in various ranges (low and high) from zero to 1 SI provides equally valid inversion models and suggest that, in practice, the procedure can only provide relative, rather than absolute, assessments of susceptibility values for this particular problem. Here we choose an inversion model obtained using distance weighting that provided an adequate fit to the data with a resulting absolute median misfit value of 0.63 nT. Of the 35140 data points only 878 (2% of the data) have misfits in excess of 5 nT. The absolute values of the model misfits are shown, using a linear colour scale from +2 to -2 nT, in Figure 9b. Portions of the spatial jitter in the image are likely to be due to spatial aliasing resulting from the 5 km data sampling used. Elsewhere a series of spatially extensive absolute misfits (the misfit used is the observed data minus that predicted by the inversion model) can be observed particularly across the SUT (Southern Upland Terrain) and extending southwards into onshore northern England. These misfits are however largely within the error assignment of +/-2 nT.

The unconstrained inversion model provides magnetic susceptibility values ranging from 0.00017 to 0.215 SI with a median value of 0.011 SI. Model cells (voxels) within the NE and SW 'no data' corners have been omitted. The continuous volumetric susceptibility model is difficult to display in a planar view. In order to compare the idealised deep body source locations ($TDR \geq 0$) obtained from the MAG0 data (Fig. 7) with the results of 3D inversion, the 3D model has been simplified to provide summary planar information. It should again be noted that the idealised bodies are associated with an assessment of the upper surfaces of isolated bodies of enhanced susceptibility. Horizontal depth

slices through the model were summed and normalised (to obtain average susceptibilities) within the depth ranges 0-10, 10-20 and 20-30 km. These are shown using a common logarithmic colour scale in Figure 10 with an overlay of the MAG0-TDR idealised bodies. The upper crustal distribution (Fig. 10a) is characterised by an extensive area of lower values (< 0.01 SI) largely towards the east and slightly elevated values (< 0.02 SI) in the west. Onshore, moderately elevated values > 0.02 SI are observed in association with the Charnwood Terrane (CT, Fig. 1), the Midland Valley Terrane (MVT, Fig. 1) and across the Laurentian Foreland in the north. The model identifies the largest upper-crustal susceptibilities across the geometrically-acute southern margin of the Hebridean Terrane, previously noted and labelled in Figure 8b. Elsewhere it can be noted that a significant number of the idealised bodies are associated with low upper crustal susceptibilities (< 0.01 SI) implying a deeper seated, higher susceptibility source.

At mid-crustal depths (Fig. 10b) the broad amplitude level of the susceptibility distribution is found to increase. The largest mid-crustal amplitude anomaly to the south of the Laurentian foreland is the Snowdon-centred anomaly (labelled S in Fig. 10b). At mid-crustal depths we observe the highest consistency between the outlines of the idealised bodies and areas of enhanced susceptibility. The outlines of the anomaly within the Midland Valley Terrane (MVT, Fig. 1) and the anomaly associated with the Charnwood Terrane (CT, Fig. 1) are particularly well-defined in the 3D model. Both of these idealised bodies are also associated with enhanced susceptibilities at all crustal levels (Figs. 10a,b,c). We also note a number of idealised bodies in the east (largely offshore) show no association with enhanced susceptibilities in the 3D model either at shallow (Fig. 10a) or mid-crustal depths (Fig. 10b). These bodies are in fact associated with some of the smallest amplitude responses in the MAG0 response (discussed later, see Fig. 11). At lower-crustal depths (Fig. 10c) the broad amplitude level of the susceptibility distribution again increases. A number of the idealised bodies exhibit more extensive and higher elevated susceptibilities in excess of ~ 0.035 SI. The most noticeable increases in lower crustal values take place within the idealised bodies spatially correlated with the Great Glen Fault (GGF, Fig. 1) and the Charnwood Terrane.

The MAG0-TDR higher susceptibility idealised basement bodies are identified irrespective of their amplitude and depth but have been obtained by a spectral decomposition applied to the whole data set. We have already noted some of the limitations of the approach in the presence of large amplitude short wavelength contributions (e.g. Fig. 6). An exact correspondence between these bodies and the 3D continuous model is an unlikely outcome. One of the main findings of the investigation is the higher level of association between the isolated, body geometries and enhanced 3D susceptibilities at depths in excess of 10 km.

4 DISCUSSION

The zero contour of the TDR function has been used to define the magnetic body edges associated with the deep magnetic response defined by MAG0. The TDR interval from zero to 90° is then used to define the extent of the more highly magnetic bodies. The TDR structural outline of deep crustal magnetic bodies obtained for the MAG0 data set is shown in Figure 11a using grey infill. A large number of the magnetic zones have previously been discussed in the literature; although not all in a deep crustal context. We have identified 30 of the zones and provide names, comments and references that assist with their interpretation in a wider context. Figure 11a shows the codes associated with the features. The image uses a background of the MAG0 response (Fig. 4d) to

indicate the variation of the low value magnetic field that separates the positively magnetised bodies. Table 3 summarises the names and codes and provides brief comments on each of the bodies. Three of the zones (IS, SNS and W) are associated with magnetic lows.

TABLE 3

The TDR response, used to define the bodies in Figure 11a, embodies an automatic gain function by virtue of the arctangent function. This means that all bodies, irrespective of response amplitude, are identified and located. The TDR function therefore equalises the contributions of small amplitude sources. In order to reintroduce the amplitude of the sources we take only the MAG0 data within the positive zone of the TDR response and regrid these data to generate the field variations associated with the bodies. Figure 11b shows the resulting magnetic field using a linear scale. The largest magnetic field variations (> 250 nT) are observed at a series of localities largely within Laurentia (i.e. to the north of the SUT). The largest amplitude feature is observed to the NW of Shetland and is associated with a localised high susceptibility zone occupying the upper crustal volume (Fig. 10). A similar but larger scale upper crustal zone was also resolved by the 3D model (Fig. 10) and is associated with the Inner Hebrides (IH) area. Within Avalonia, the Snowdon-centred anomaly in North Wales and the South Central England (SCE) anomaly display the largest amplitudes.

4.1 Sources of long-wavelength magnetic anomalies over northern (Laurentian) Britain

Strong magnetic anomalies over the central and southern parts of the Lewisian Gneiss Complex in the Ullapool area (U, Fig. 11a) are known to occur over Archaean granulite facies units (Powell 1970; Bott *et al.* 1972). Piper (1992) described an increase in magnetisation associated with Palaeoproterozoic (Laxfordian) reworking, but the values quoted (mean volume susceptibilities of the order of 0.001 SI) suggest that the most magnetic parts of the complex have not been sampled (much higher magnetic susceptibilities are reported by Coats *et al.* (1997) and Rollin (2009)). There is a spatial correlation between Laxfordian amphibolite facies shear zones and relative magnetic lows over the complex. A substantial increase in rock magnetisation across the transition from amphibolite to granulite facies gneisses has also been reported in northern Norway (Olesen *et al.* 1991), southern India (Piper *et al.* 2003) and West Greenland (Korstgård *et al.* 2006), and is compatible with magnetic property data from lower crustal xenoliths (Wasilewski & Mayhew 1982, 1992).

It is thus likely that the oldest (Archaean) basement beneath northern Britain is relatively magnetic, and this also applies to younger magmatic rocks that were accreted during Palaeoproterozoic orogenesis. The mafic rocks of the South Harris Complex are highly magnetic (Westbrook 1974), and are inferred to be part of a Palaeoproterozoic arc dated at c. 1890 Ma (Mason *et al.* 2004). The arc magmatic rocks of the CWIT-Rhinns Terrane (Fig. 1) are associated with strong magnetic anomalies over Stanton Banks and the southern Inner Hebrides (SB and IH in Fig. 11a). These have typical crystallisation ages of 1780 - 1800 Ma (Marcantonio *et al.* 1988; Daly *et al.* 1991; Scanlon *et al.* 2003; Ritchie *et al.* 2013). They form part of a belt of Palaeoproterozoic arc-related rocks associated with the formation of the Columbia (or Nuna) supercontinent (Zhao *et al.* 2004; Rogers & Santosh 2002, 2009). To the west this includes the major Julianeåb batholith within the Ketilidean orogen of southern Greenland (Garde *et al.* 2002) and the plutonic suites of the Cape Harrison Domain in the laterally equivalent Makkovik Orogen of Labrador (Kerr *et al.* 1997). To the east, Palaeoproterozoic

magnetic plutonic rocks of the Transscandinavian Igneous Belt are responsible for conspicuous magnetic anomalies in the Svecofennian Orogen (Mansfield 1995, Ebbing *et al.* 2012). Given this continuity, it appears likely that similar rocks may occur beneath the Dalradian metasediments of the northern part of the Grampian Terrane (CHGT, Fig. 1). There is evidence to support this in granite inheritance (Dicken & Bowes 1991) and from sedimentary provenance studies (Banks *et al.* 2013). Magnetic evidence for such an extension include the conspicuous anomaly along the Great Glen Fault (which may include contributions from both Lewisian and CWIT-Rhinns basement sources) and an anomaly extending offshore from the Lossiemouth area (Rollin 2009) (GG and L respectively in Figure 11a).

The Midland Valley Terrane is underpinned by an Ordovician arc complex formed at very different (Laurentian) latitudes (Bluck 2013), and it is possible that long wavelength magnetic anomalies in this area and offshore Stonehaven (MV and ST in Figure 11a) reflect this (although shallow Upper Palaeozoic volcanic rocks are also responsible for magnetic anomalies in the area).

4.2 Sources of long-wavelength magnetic anomalies over southern (Eastern Avalonian) Britain

Long-wavelength magnetic anomalies over southern Britain have been linked to a Neoproterozoic (Eastern Avalonian) crystalline basement formed at the margin of Gondwana (Kimbell & Quirk 1999; Kimbell *et al.* 2006). Again, the magnetic anomalies appear to be linked to calc-alkaline magmatic rocks, and analogues have been identified in the Newfoundland (Western Avalonia) area (Haworth & Lefort 1979). The South Central England (SCE) magnetic anomaly can be modelled as Precambrian magnetic basement which becomes buried southwards by north-vergent Variscan thrusting (Busby *et al.* 2006). This Precambrian basement is part of Avalonian basement of the Midlands Microcraton and may represent the oldest basement fragment in the area. It has been suggested that the long wavelength Galloway and Berwickshire magnetic anomalies over southern Scotland (G and BE in Fig. 11a) are associated with fragments of Avalonian crystalline basement thrust beneath the Southern Uplands accretionary prism (Kimbell & Stone 1995), and a similar explanation may extend to the source of the Virginia anomaly beneath Ireland (V in Fig. 11a). This accretion preceded final oceanic closure along the NE-trending Iapetus Suture just to the south of these fragments (IS in Fig. 11a). A relative magnetic low over the suture is interpreted to be due to less magnetic metasedimentary rocks sandwiched between the crystalline basement blocks in the convergence zone (Kimbell & Stone 1995; Kimbell & Quirk 1999). A long-wavelength, NW-trending magnetic low beneath the Southern North Sea (SNS, Fig. 11a) may be associated with the Tornquist convergence zone in an analogous fashion. The NW-trending Furness-Norfolk and Derby – St Ives magnetic anomalies (FN and DSI in Fig. 11a) appear to be caused by the products of Ordovician arc magmatism associated with the south-westward subduction of the Tornquist Ocean (Pharaoh *et al.* 1993). Finally, there is a distinct magnetic boundary along the Variscan front in southern Britain indicative of the burial of magnetic basement of the Midlands Microcraton beneath less magnetic rocks carried by northward-verging Variscan thrusts (Busby & Smith 2001).

5 CONCLUSIONS

The study has provided a coherent assessment of the deep crustal magnetic bodies responsible for the long wavelength magnetic features observed across Britain and eastern Ireland. The simplest description of the long-wavelength magnetic features is obtained through upward-continuation

filtering of the data to elevations above 50 km. At these levels, two large scale positively magnetised zones are observed in association with Laurentia in the north and with Avalonia in the south. The lateral boundaries of the southern zone show an approximate and partial coincidence with terrane boundaries. The observed south-western limb associated with the northern zone was subsequently modelled as a large-scale upper crustal feature associated with the Southern Inner Hebrides area.

Spectral decomposition of the data has clearly revealed some intense, high-amplitude, shallow features to the NW of the Southern Upland Terrane. Some of these features prove problematic when attempting to extract deeper basement information. The spatial form of the basement (lower half-space) magnetic field (MAG0) extracted by spectral decomposition was found to provide a simplified anomaly distribution that could be associated with a conceptual model of idealised, deep-seated, magnetised basement bodies. The MAG0 data set provides a simplified and idealised assessment of deep source bodies across the whole study area in map form.

In order to further assess the definition of the idealised bodies and their associated depths we have carried out an unprejudiced (largely unconstrained) 3D inversion of the data. Both the idealised body analysis and the inversion modelling assume normally-magnetised material. The susceptibilities returned by the inversion are probably best considered as relative rather than absolute. The inversion is carried out at a coarse scale but is sufficient to assess deep and shallow contributions at the crustal scale. A large central area of the 3D model, separating Laurentia and Avalonia, is characterised by relatively low values of susceptibility (<0.020 SI) throughout the whole crustal volume.

The 3D model of subsurface susceptibilities obtained is an inherently smooth and continuous distribution so the comparison with the idealised basement features can only be achieved in an approximate manner by isolating higher susceptibility zones within the 3D model space. Across the valid model region we find that the MAG0-TDR basement bodies are largely consistent with relatively high susceptibility zones (e.g. > 0.0075 SI) at depths in excess of 10 km within the 3D model. The 3D model also identifies three localised high susceptibility zones occupying the upper crustal volume (0 to 10 km). The two main bodies occur to the west of Shetland and, more extensively, across the Inner Hebrides area.

At each stage of the analysis, the high susceptibility bodies detected have been compared with the tectonic framework of Britain using existing definitions of the crustal terranes. Inevitably a number of the magnetic zones identified have been previously discussed in the literature, although not all in a specific deep crustal context. A lexicon of the bodies is provided, based on existing references. The long-wavelength magnetic anomalies over Britain provide an insight into the way the different basement elements have been assembled into their present-day configuration. In the north is the Archaean magnetic basement of Laurentia onto which have been accreted magnetic rocks of Palaeoproterozoic (CWIT-Rhinns Terrane), Ordovician (Midland Valley Terrane) and Neoproterozoic (sub-Southern Upland) origin. Magnetic anomalies record the assembly of the Gondwanan (Eastern Avalonian) part of the country through Neoproterozoic and Ordovician (Tornquist) arc magmatism and accretion. The convergence zones between Laurentia, Avalonia and Baltica have all left a magnetic imprint, as has Variscan convergence to the south.

ACKNOWLEDGEMENTS

The study used a composite airborne and marine magnetic data set collected by a number of organisations. The relevant data sources are a subset of those used in the published magnetic anomaly map at a scale of 1:1.5M and described by British Geological Survey (1998). The data from the Republic of Ireland are copyright Geological Survey of Ireland. We thank Dave Schofield for his internal review. This paper is published with the permission of the Executive Director, British Geological Survey (NERC).

REFERENCES

- Allen, P.M. & Jackson, A.A., 1985. Geology of the country around Harlech. *Memoir of the British Geological Survey*, sheet 149 (England & Wales).
- Allsop, J.M., 1987. Patterns of late Caledonian intrusive activity in eastern and northern England from geophysics, radiometric dating and basement geology, *Proceedings of the Yorkshire Geological Society*, **46**, 335-353.
- Banks, C.J., Peters, D.P., Winchester, J.A., Noble, S.R. & Horstwood, M.S.A., 2013. Basement palaeogeography of late Neoproterozoic Scotland: constraints from exotic clasts within the lower Dalradian Supergroup, *Scottish Journal of Geology*, **49**, 81-92.
- Beamish, D. & White, J.C., 2011. Aeromagnetic data in the UK: a study of the information content of baseline and modern surveys across Anglesey, North Wales, *Geophysical Journal Int.*, **184**, 171-190.
- Blakely, R.J., 1995. *Potential Theory in Gravity and Magnetic Applications*, Cambridge University Press, Cambridge, United Kingdom.
- Blakely, R.J., Brocher, T.M. & Wells, R.E., 2005. Subduction-zone magnetic anomalies and implications for hydrated forearc mantle, *Geology*, **33**, 445-448.
- Bluck, B.J., 2013. Geotectonic evolution of Midland Scotland from Cambrian to Silurian: a review, *Scottish Journal of Geology*, **49**, 105-116.
- Bott, M.H.P., Holland, J.G., Storry, P.G. & Watts, A.B., 1972. Geophysical evidence concerning the structure of the Lewisian of Sutherland, N.W. Scotland, *Journal of the Geological Society*, **128**, 599-610.
- British Geological Survey, 1998. Colour-shaded Relief Magnetic Anomaly Map of Britain, Ireland and adjacent areas. Royles, C.P and Smith, I.F. (compilers) 1:1 500 000 scale. British Geological Survey, Keyworth, Nottingham, UK.
- Busby, J.P., Kimbell, G.S. & Pharaoh, T.C., 1993. Integrated geophysical/geological modelling of the Caledonian and Precambrian basement of southern Britain, *Geological Magazine*, **130**, 593-604.

- Busby, J.P. & Smith, N.J.P., 2001. The nature of the Variscan basement in southeast England: evidence from integrated potential field modelling, *Geological Magazine*, **138**, 669-685.
- Busby, J.P., Walker, A.S.D. & Rollin, K.E., 2006. *Regional Geophysics of South-east England*. Version 1.0. on CD-ROM (Keyworth, Nottingham: British Geological Survey).
- Coats, J.S., Shaw, M.H., Gunn, A.G., Rollin, K.E. & Fortey, N.J., 1997. Mineral exploration in Lewisian supracrustal and basic rocks of the Scottish Highlands and Islands. *British Geological Survey Mineral Reconnaissance Programme Report*, No. 146.
- Cooper, G.R.J & Cowan, D.R., 2006, Enhancing potential field data using filters based on the local phase, *Computers and Geosciences*, **32**, 1585–1591.
- Cornwell, J.D. & Cave, R., 1986. An airborne geophysical survey of part of west Dyfed, South Wales, and some related ground surveys. *British Geological Survey Mineral Reconnaissance Programme Report*, No. 84.
- Cornwell, J.D. & Walker, A.S.D., 1989. Regional Geophysics in *Metallogenic models and exploration criteria for buried carbonate-hosted ore deposits : a multidisciplinary study in eastern England*, pp. 25-51, eds Plant, J.A. & Jones, D.G., Institute of Mining and Metallurgy, London and British Geological Survey, Keyworth, Nottingham.
- Daly, J.S., Muir, R.J. & Cliff, R.A., 1991. A precise U-Pb zircon age for the Inishtrahull syenitic gneiss, County Donegal, Ireland, *Journal of the Geological Society*, **148**, 639-642.
- Dickin, A.P. & Bowes, D.R., 1991. Isotopic evidence for the extent of early Proterozoic basement in Scotland and northwest Ireland, *Geological Magazine*, **128**, 385-388.
- Donato, J.A., Martindale, W. & Tully, M.C., 1983. Buried granites within the Mid North Sea High, *Journal of the Geological Society*, **140**, 825-837.
- Donato, J.A. & Tully, M.C., 1982. A proposed granite batholith along the western flank of the North Sea Viking Graben, *Geophysical Journal of the Royal Astronomical Society*, **69**, 187-195.
- Ebbing, J., England, R.W., Korja, T., Lauritsen, T., Olesen, O., Stratford, W. & Weidle, C., 2012. Structure of the Scandes lithosphere from surface to depth, *Tectonophysics*, **536-537**, 1-24.
- Fairhead, J.D., Green, C.M., Verduzco, B. & Mackenzie, C., 2004. A new set of magnetic field derivatives for mapping mineral prospects. *ASEG 17th Geophysical Conference and Exhibition*, Sydney, Australia, Extended Abstracts.
- Fedi, M., Florio, G. and Cascone, L., 2012. Multiscale analysis of potential fields by a ridge consistency criterion: the reconstruction of the Bishop basement, *Geophysical Journal Int.*, **188**, 103-114.
- Ferré, E.C., Friedman, S.A., Martín-Hernández, F., Feinberg, J.M., Conder, J.A. & Ionov, D.A., 2013. The magnetism of mantle xenoliths and potential implications for sub-Moho magnetic sources, *Geophysical Research Letters*, **40**, 105-110.

Ferré, E.C., Friedman, S.A., Martín-Hernández, F., Feinberg, J.M., Till, J.L., Ionov, D.A. & Conder, J.A., 2014. Eight good reasons why the uppermost mantle could be magnetic, *Tectonophysics*, **624–625**, 3-14.

Flanagan, G. & Bain, J.E., 2013. Improvements in magnetic depth estimation: application of depth and width extent nomographs to standard depth estimation techniques, *First Break*, **31**, 41-51.

Garde, A.A., Chadwick, B., Grocott, J., Hamilton, M.A., McCaffrey, K.J.W. & Swager, C.P., 2002. Mid-crustal partitioning and attachment during oblique convergence in an arc system, Palaeoproterozoic Ketilidian orogen, southern Greenland, *Journal of the Geological Society*, **159**, 247-261.

Goodenough, K.M., Crowley, Q.G., Krabbendam, M. & Parry, S.F. 2013. New U-Pb age constraints for the Laxford Shear Zone, NW Scotland: Evidence for tectonomagmatic processes associated with the formation of a Paleoproterozoic supercontinent, *Precambrian Research*, **233**, 1-19.

Goodwin, J.A., Hackney, R. & Williams, N.C. 2015. 3D Geophysical inversion modelling of the Wallaby Plateau: evidence for continental crust and seaward-dipping reflectors. Record 2015/01. Geoscience Australia, Canberra. <http://dx.doi.org/10.11636/Record.2015.001>.

Hall, J. & Al-Haddad, F.M., 1979. Variation of effective seismic velocities of minerals with pressure and its use in velocity prediction, *Geophysical Journal of the Royal Astronomical Society*, **57**, 107-118.

Haworth, R.T. & Lefort, J.P., 1979. Geophysical evidence for the extent of the Avalon zone in Atlantic Canada, *Canadian Journal of Earth Sciences*, **16**, 552-567.

Holloway, S., Reay, D.M., Donato, J.A. & Beddoe-Stephens, B., 1991. Distribution of granite and possible Devonian sediments in part of the East Shetland Platform, North Sea, *Journal of the Geological Society*, **148**, 635-638.

Howells, M.F. & Smith, M., 1997. Geology of the country around Snowdon. *Memoir of the British Geological Survey*, Sheet 119 (England & Wales).

Kearey, P., 1991. A possible basaltic deep source of the south-central England magnetic anomaly, *Journal of the Geological Society*, **148**, 775-780.

Kerr, A., Hall, J., Wardle, R.J., Gower, C.F. & Ryan, B., 1997. New reflections on the structure and evolution of the Makkovikian - Ketilidian Orogen in Labrador and southern Greenland, *Tectonics*, **16**, 942-965.

Kimbell, G.S., Carruthers, R.M., Walker, A.S.D. & Williamson, J.P., 2006. *Regional geophysics of southern Scotland and Northern England*, Version 1.0 on CD-ROM, British Geological Survey, Keyworth, Nottingham.

Kimbell, G.S. & Quirk, D.G., 1999. Crustal magnetic structure of the Irish Sea region: evidence for a major basement boundary beneath the Isle of Man, *Geological Society, London, Special Publications*, **160**, 227-238.

Kimbell, G.S. & Stone, P., 1995. Crustal magnetization variations across the Iapetus Suture Zone, *Geological Magazine*, **132**, 599-609.

- Kimbell, G.S., Young, B., Millward, D. & Crowley, Q.G., 2010. The North Pennine batholith (Weardale Granite) of northern England: new data on its age and form, *Proceedings of the Yorkshire Geological Society*, **58**, 107-128.
- Korstgård, J.A., Stensgaard, B.M. & Rasmussen, T.M., 2006. Magnetic anomalies and metamorphic boundaries in the southern Nagssugtoqidian orogen, West Greenland, *Bulletin of the Geological Survey of Denmark and Greenland*, **11**, 179-184.
- Lee, M.K., Pharaoh, T.C. & Soper, N.J., 1990. Structural trends in central Britain from images of gravity and aeromagnetic fields, *Journal of the Geological Society*, **147**, 241-258.
- Lee, M.K., Pharaoh, T.C., Williamson, J.P., Green, C.A. & De Vos, W., 1993. Evidence on the deep structure of the Anglo-Brabant Massif from gravity and magnetic data, *Geological Magazine*, **130**, 575-582.
- Li, X., 2003. On the use of different methods for estimating magnetic depth, *The Leading Edge*, **22**, 1090-1099.
- Li, Y. & Oldenburg, D. W., 1996, 3-D inversion of magnetic data. *Geophysics*, **61**, 394--408.
- Lyngsø, S. B., Thybo, H., Rasmussen, T. M., 2006. Regional geological and tectonic structures of the North Sea area from potential field modelling, *Tectonophysics*, **413**, 147-170.
- Mansfeld, J., 1995. *Crustal evolution in the southeastern part of the Fennoscandian Shield*. Unpublished PhD Thesis, Stockholm University.
- Marcantonio, F., Dickin, A.P., McNutt, R.H. & Heaman, L.M., 1988. A 1,800-million-year-old Proterozoic gneiss terrane in Islay with implications for the crustal structure and evolution of Britain, *Nature*, **335**, 62-64.
- Mason, A.J., Parrish, R.R. & Brewer, T.S., 2004. U–Pb geochronology of Lewisian orthogneisses in the Outer Hebrides, Scotland: implications for the tectonic setting and correlation of the South Harris Complex, *Journal of the Geological Society, London*, **161**, 45-54.
- Miles, A., Graham, C., Hawkesworth, C., Gillespie, M., Dhuime, B. & Hinton, R., 2014. Using Zircon Isotope Compositions to Constrain Crustal Structure and Pluton Evolution: the Iapetus Suture Zone Granites in Northern Britain, *Journal of Petrology*, **55**, 181-207.
- Miller, H.G. & Singh, V., 1994. Potential field tilt - A new concept for location of potential field sources, *Journal of Applied Geophysics*, **32**, 213–217.
- Morris, P. & Max, M.D., 1995. Magnetic crustal character in Central Ireland, *Geological Journal*, **30**, 49-67.
- Nabighian, M.N., Grauch, V.J.S., Hansen, R.O., LaFehr, T.R., Li, Y., Peirce, J.W., Phillips, J.D. & Ruder, M.E., 2005. The historical development of the magnetic method in exploration, *Geophysics*, **70**, 33-61.

- Olesen, O., Henkel, H., Kaada, K. & Tveten, E., 1991. Petrophysical properties of a prograde amphibolite-granulite facies transition zone at Sigerfjord, Vesterålen, northern Norway, *Tectonophysics*, **192**, 33-39.
- Pedersen, L.B., 1991. Relations between potential fields and some equivalent sources, *Geophysics*, **56**, 961-971.
- Pharaoh, T.C., 1999. Palaeozoic terranes and their lithospheric boundaries within the Trans-European Suture Zone (TESZ): a review, *Tectonophysics*, **314**, 17-41.
- Pharaoh, T., England, R. & Lee, M., 1995. The concealed Caledonide basement of Eastern England and the southern North Sea - a review, *Stud. Geophys. Geod.*, **39**, 330-346.
- Pharaoh, T.C., Brewer, T.S. & Webb, P.C., 1993. Subduction-related magmatism of late Ordovician age in eastern England, *Geological Magazine*, **130**, 647-656.
- Pharaoh, T.C., Morris, J., Long, C.B. & Ryan, P.D. 1996. *The Tectonic Map of Britain, Ireland and adjacent areas. Sheet 1. 1:1 500 000 Scale*. British Geological Survey and Geological Survey of Ireland.
- Phillips, E.R., Evans, J.A., Stone, P., Horstwood, M.S.A., Floyd, J.D., Smith, R.A., Akhurst, M.C. & Barron, H.F., 2003. Detrital Avalonian zircons in the Laurentian Southern Uplands terrane, Scotland, *Geology*, **31**, 625-628.
- Phillips, J. D., 2001. Designing matched bandpass and azimuthal filters for the separation of potential field anomalies by source region and source type, *ASEG 15th Geophysical Conference and Exhibition*, Extended Abstracts.
- Piper, J.D.A., 1992. Post-Laxfordian magnetic imprint in the Lewisian metamorphic complex and strike-slip motion in the Minches, NW Scotland, *Journal of the Geological Society*, **149**, 127-137.
- Piper, J.D.A., Mallik, S.B., Bandyopadhyay, G., Mondal, S. & Das, A.K., 2003. Palaeomagnetic and rock magnetic study of a deeply exposed continental section in the Charnockite Belt of southern India: implications to crustal magnetisation and palaeoproterozoic continental nuclei, *Precambrian Research*, **121**, 185-219.
- Powell, D.W., 1970. Magnetised rocks within the Lewisian of Western Scotland and under the Southern Uplands, *Scottish Journal of Geology*, **6**, 353-369.
- Pratt, W.T., Woodhall, D.G., Howells, M.F., Leng, M.J., Cave, R., Scott, M.S., Carruthers, R.M., Molyneux, S.G., Rushton, A.W.A. & Zalasiewicz, J.A., 1995. Geology of the country around Cadair Idris. *Memoir of the British Geological Survey* sheet 149 (England & Wales).
- Reid, A.B. & Thurston, J.B., 2014. The structural index in gravity and magnetic interpretation: errors, uses and abuses, *Geophysics*, **79**, 161-166.
- Ritchie, J.D., Swallow, J.L., Mitchell, J.G. & Morton, A.C., 1988. Jurassic ages from intrusives and extrusives within the Forties igneous province, *Scottish Journal of Geology*, **24**, 81-88.

- Ritchie, J.D., Ziska, H., Johnson, H., Evans, D. (editors), 2011. *Geology of the Faroe-Shetland Basin and adjacent areas*. British Geological Survey Research Report RR/11/01.
- Ritchie, J.D., Noble, S., Darbyshire, F., & Chambers, L. 2013. Precambrian basement, in *Geology of the Rockall Basin and adjacent areas*, pp. 47-53, eds. Hitchen, K., Johnson, H. & Gatliff, R.W., British Geological Survey Research Report RR/12/03.
- Rogers, J.J.W. & Santosh, M., 2002. Configuration of Columbia, a Mesoproterozoic Supercontinent, *Gondwana Research*, **5**, 5-22.
- Rogers, J.J.W. & Santosh, M., 2009. Tectonics and surface effects of the supercontinent Columbia, *Gondwana Research*, **15**, 373-380.
- Rollin, K.E., 2009. *Regional geophysics of Northern Scotland*, Version 1.0 on CD-ROM, British Geological Survey, Keyworth, Nottingham.
- Salem, A., Ravat, D., Smith, R.S. & Ushijima, K., 2005. Interpretation of magnetic data using an enhanced local wavenumber (ELW) method, *Geophysics*, **70**, L7-L12.
- Salem, A., Williams, S., Fairhead, J.D., Ravat, D. & Smith, R.S., 2007. Tilt-depth method: A simple depth estimation method using first-order magnetic derivatives, *The Leading Edge*, **26**, 1502-1505.
- Scanlon, R.P., Daly, J.S. & Whitehouse, M.J., 2003. The c.1.8 Ga Stanton Banks Terrane, offshore western Scotland, a large juvenile Palaeoproterozoic crustal block within the accretionary Lewisian Complex, *Geophysical Research Abstracts*, **5**, 13248.
- Smith, K. & Ritchie, J.D., 1993. Jurassic volcanic centres in the Central North Sea, *Geological Society, London, Petroleum Geology Conference series*, **4**, 519-531.
- Soper, N.J., England, R.W., Snyder, D.B. & Ryan, P.D., 1992. The Iapetus suture zone in England, Scotland and eastern Ireland: a reconciliation of geological and deep seismic data, *Journal of the Geological Society, London*, **149**, 697-700.
- Spector, A. & Grant, F.S. 1970. Statistical methods for interpreting aeromagnetic data, *Geophysics*, **35**, 293-302.
- Spicer, B., Morris, B. & Ugalde, H., 2011. Structure of the Rambler Rhyolite, Baie Verte Peninsula, Newfoundland: Inversions using UBC-GIF Grav3D and Mag3D. *Journal of Applied Geophysics*, **75** (1), 9-18.
- Syberg, F.J.R., 1972. A Fourier method for the regional-residual problem of potential field, *Geophysical Prospecting*, **20**, 47-75.
- Trewin, N.H. & Rollin, K.E. 2002. Geological history and structure of Scotland. in Trewin, N.H. (ed.) *Geology of Scotland*. Geological Society, London, 1-25.
- Verduzco, B., Fairhead, J.D. & Green, C.M., 2004. New insights into magnetic derivatives for structural mapping, *The Leading Edge*, **23**, 116-119.

- Waldron, J.W.F., Floyd, J.D., Simonetti, A. & Heaman, L.M., 2008. Ancient Laurentian detrital zircon in the closing Iapetus Ocean, Southern Uplands terrane, Scotland, *Geology*, **36**, 527-530.
- Waldron, J.W.F., Schofield, D.I., Dufrane, S.A., Floyd, J.D., Crowley, Q.G., Simonetti, A., Dokken, R.J. & Pothier, H.D., 2014. Ganderia-Laurentia collision in the Caledonides of Great Britain and Ireland, *Journal of the Geological Society*, **171**, 555-569.
- Wasilewski, P. & Mayhew, M.A., 1982. Crustal xenolith magnetic properties and long wavelength anomaly source requirements, *Geophysical Research Letters*, **9**, 329-332.
- Wasilewski, P.J. & Mayhew, M.A., 1992. The Moho as a magnetic boundary revisited, *Geophysical Research Letters*, **19**, 2259-2262.
- Wasilewski, P.J., Thomas, H.H. & Mayhew, M.A., 1979. The Moho as a magnetic boundary, *Geophysical Research Letters*, **6**, 541-544.
- Westbrook, G.K., 1974. The South Harris magnetic anomaly, *Proceedings of the Geologists' Association*, **85**, 1-12.
- Williamson, J.P., Pharaoh, T.C., Banka, D., Thybo, H., Laigle, M. & Lee, M.K., 2002. Potential field modelling of the Baltica-Avalonia (Thor-Tomquist) suture beneath the southern North Sea, *Tectonophysics*, **360**, 47-60.
- Wills, L.J., 1978. A Palaeogeological Map of the Lower Palaeozoic Floor below the cover of Upper Devonian, Carboniferous and Later Formations with inferred and speculative reconstructions of Lower Palaeozoic and Precambrian outcrops in adjacent areas, *Geological Society, London, Memoirs*, **8**, 9-34.
- Winchester, J.A. & Max, M.D., 1982. The geochemistry and origins of the Precambrian rocks of the Rosslare Complex, SE Ireland, *Journal of the Geological Society*, **139**, 309-319.
- Zhao, G., Sun, M., Wilde, S.A. & Li, S., 2004. A Paleo-Mesoproterozoic supercontinent: assembly, growth and breakup, *Earth-Science Reviews*, **67**, 91-123.

Table 1. The 15 terranes and 2 subterranes that define the tectonic framework of Britain and eastern Ireland.

LABEL	Terrane	Age of crustal formation
BsT	Bellewstown Sub-terrane	?Ordovician
CHGT	Central Highlands Terrane (Grampian Terrane)	Proterozoic
CSB	Caledonides of Southern Britain	Neoproterozoic
SUT	Southern Uplands Terrane	Ordovician
CT	Charnwood Terrane	Neoproterozoic
CWIT	Colonsay - W Islay - Inishtrahull Terrane (Rhinn's Terrane)	Palaeoproterozoic
GsT	Grangegeeth Sub-terrane	?Ordovician
HT	Hebridean Terrane	Archaean
LLT	Leinster-Lakesman Terrane	Ordovician
MVT	Midland Valley Terrane	?Mesoproterozoic
NAT	North Armorican Composite Terrane (east)	Archaean-Proterozoic
NHT	Northern Highlands Terrane	Archaean
NT	Normannian Terrane	Neoproterozoic
RMT	Rosslare-Monian Terranes	Neoproterozoic

SNST	Southern North Sea Terrane	?Ordovician
VRZ	Variscide Rhenohercynian Zone	Neoproterozoic
WT	Wrekin Terrane	Neoproterozoic

Table 2. Simple statistics of magnetic fields obtained using matched band-pass filters. All values are nT.

	Spectral depth (m)	Minimum (nT)	Maximum (nT)	Mean (nT)	Standard Deviation (nT)
MAG		-3210	2512	-11.8	111.8
MAG4	407	-581	513	0.0	3.0
MAG3	1609	-1976	1690	0.0	26.6
MAG2	5018	-1550	1506	0.0	39.5
MAG1	16,630	-329	628	-0.1	35.9
MAG0	35,250	-265	604	-11.6	79.0

Table 3. Summary of 30 magnetic features identified in association with the magnetic basement analysis. All features are positive anomalies with the exception of IS, SNSD and W which are associated with magnetic lows.

Code	Name	Possible source
B	Birmingham anomaly	Plutonic core of a Neoproterozoic (Charnian) arc (Lee <i>et al.</i> 1990; Busby <i>et al.</i> 1993)
BE	Berwickshire anomaly	Underthrust magnetic basement fragment of Avalonian origin? (Kimbell & Stone 1995)
CB	Culm Basin	Mid-crustal magnetic block sandwiched between Variscan thrusts?
CW	Central Wales anomaly	Probable Precambrian source. Correlation with gravity low suggests dense Lower Palaeozoic rocks over less-dense magnetic basement.
DSI	Derby - St Ives anomaly	Ordovician intrusive rocks possibly associated with subduction of the Tornquist Ocean (Pharaoh <i>et al.</i> 1993; Allsop 1987). Cornwell & Walker (1989) suggested a Precambrian basement source.
ESH	East Shetland High	Donato & Tully (1982) suggested an association with a granite pluton but Holloway <i>et al.</i> (1991) preferred shallow magnetic basement.
FB	Fisher Bank Centre	Part of the Jurassic Forties Volcanic Province (Smith & Ritchie 1993)

FBC	Faroe Bank Channel	Palaeogene igneous centre (Faroe Bank Channel Knoll) plus longer wavelength feature to the NW associated with a deeper (Palaeogene or basement?) source
FL	Flannan anomaly	Evidence for magnetic Caledonian intrusive rocks on the Flannan High (BGS, unpublished data)
FN	Furness - Norfolk anomaly	Alternative explanations: Ordovician arc magmatism (Pharaoh <i>et al.</i> 1993, 1995); early Palaeozoic magnetic metasediments (Lee <i>et al.</i> , 1993); Precambrian basement (Wills 1978); Devonian metamorphism (Allsop 1987)
FVP	Forties Volcanic Province	Jurassic volcanic province (Ritchie <i>et al.</i> 1988; Smith & Ritchie 1993).
G	Galloway anomaly	Underthrust magnetic basement fragment of Avalonian origin? (Kimbell & Stone 1995; Phillips <i>et al.</i> 2003). See subsequent discussion by Waldron <i>et al.</i> (2008, 2014) and Miles <i>et al.</i> (2014)
GG	Great Glen anomaly	The form of the anomaly requires a magnetic basement high straddling the line of the Great Glen Fault. This possibly reflects a combination of Lewisian and younger (Rhinn's age) sources (Rollin 2009)
IH	Inner Hebrides	Granulite facies Lewisian basement (includes magnetite-rich gneisses on Tiree; Coats <i>et al.</i> 1997). Magnetic signatures in this region strongly affected by Palaeogene igneous rocks.
IRS	Irish Sea	Magnetic Avalonian basement (Kimbell & Quirk 1999)
IS	Iapetus Suture	Magnetic low caused by less magnetic metasedimentary rocks (originally deposited on Ordovician margins) sandwiched between magnetic basement blocks (Kimbell & Stone 1995; Kimbell & Quirk 1999)
L	Lossiemouth anomaly	Palaeoproterozoic magnetic basement (Rollin 2009)
MNSH	Mid North Sea High	Magnetic granite (Dogger Granite) probably of late Caledonian age (Donato <i>et al.</i> 1983)
MV	Midland Valley	Region contains numerous, shallow Upper Palaeozoic magnetic sources, possibly underlain by deeper sources associated Ordovician arc magmatism (Rollin 2009).
RNW	Rosslare - North Wales anomaly	In the North Wales area, shallow magnetic Cambrian strata (Rhinog and Dolwen formations) overlie a deeper, probably Precambrian source (Allen & Jackson 1985; Pratt <i>et al.</i> 1995; Howells & Smith 1997). The age of the Rosslare gneisses is not known, but they have a complex metamorphic history which predates intrusions dated at 650 Ma (Winchester & Max 1982).
SB	Stanton Banks anomaly	Magnetic, calc-alkaline Palaeoproterozoic rocks of the CWIT (Rhinn's) Terrane (Ritchie <i>et al.</i> 2013)
SCE	South Central England magnetic anomaly	Deep Variscan basaltic source suggested by Kearey (1991). Precambrian crystalline basement suggested by Busby <i>et al.</i> (1993), Busby & Smith 2001)
SD	Strath Dionard anomaly	Bott <i>et al.</i> (1972) suggested magnetic Scourian gneiss at shallow depth but this was not supported by a seismic refraction experiment (Hall & Al-Haddad 1979). Alternative explanations are a buried magnetic granite (Powell 1970) or the cumulative effect of magnetic pegmatite-granite veins (Rollin 2009)
SNS	Southern North Sea	Low crustal magnetisation beneath the Southern North Sea (Williamson <i>et al.</i> 2002; Kimbell <i>et al.</i> 2006)

ST	Stonehaven anomaly	Coincident with gravity high suggesting a basic mass within the Midland Valley terrane or within Dalradian rocks thrust beneath the HBF (Rollin 2009)
SW	South Wales anomalies	Precambrian sources, typically in the cores of anticlines (e.g. Cornwell & Cave 1986). Some shallow Lower Palaeozoic magnetic units (Skomer Volcanic Group and Fishguard Volcanic Group).
U	Ullapool area	Magnetic anomalies associated with granulite facies Lewisian gneisses in the central part of the Lewisian Gneiss Complex. Distinct contrast with the less magnetic amphibolite facies rocks south of the Gruinard Front (Powell 1970; Bott <i>et al.</i> 1972).
V	Virginia anomaly	Magnetic basement block in the hanging wall of the Iapetus Suture Zone (Morris & Max 1995; Kimbell & Stone 1995; Kimbell & Quirk 1999).
W	Weardale anomaly	Magnetic low over the North Pennine (Weardale) Granite, implying that magnetic Avalonian basement extends northwards beneath the Alston Block and has been modified (punctured and/or demagnetised) as a result of its intrusion (Kimbell <i>et al.</i> 2010).
WOS	West of Shetland anomalies	Clear correlation with structural highs in magnetic Lewisian basement (e.g. Ritchie <i>et al.</i> 2011)

FIGURES

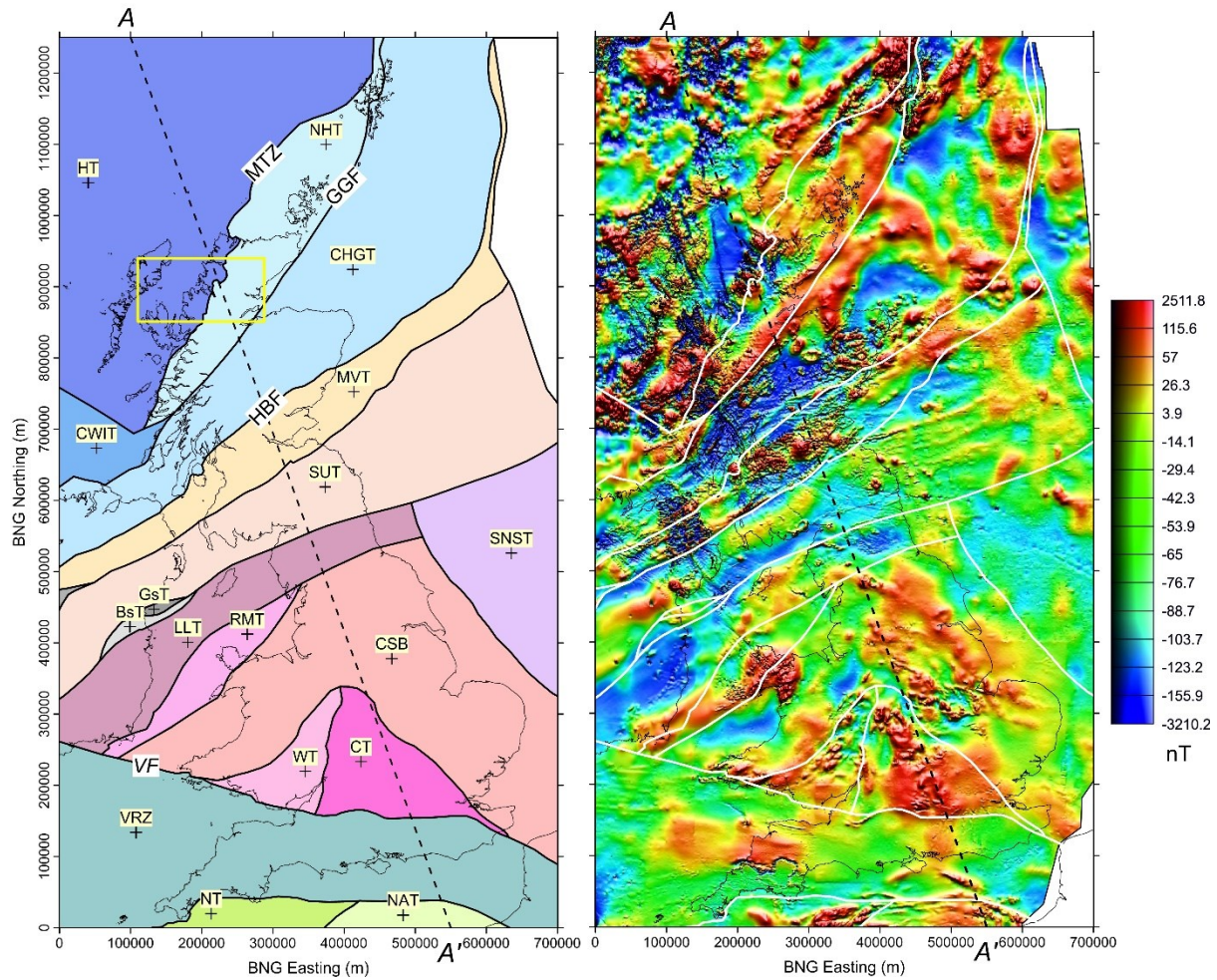


Figure 1. The study area (700 x 1250 km) with a profile line A-A' identified. Labelled and coloured tectonic terranes (see Table 1) with 4 boundaries identified as MTZ (Moine Thrust Zone), GGF (Great Glen Fault), HBF (Highland Boundary Fault) and VF (Variscan Front). BNG refers to British National Grid coordinates which are used throughout this study. The yellow box shows the Hebridean study area (178 x 105 km) discussed in the text and shown in Fig. 2.

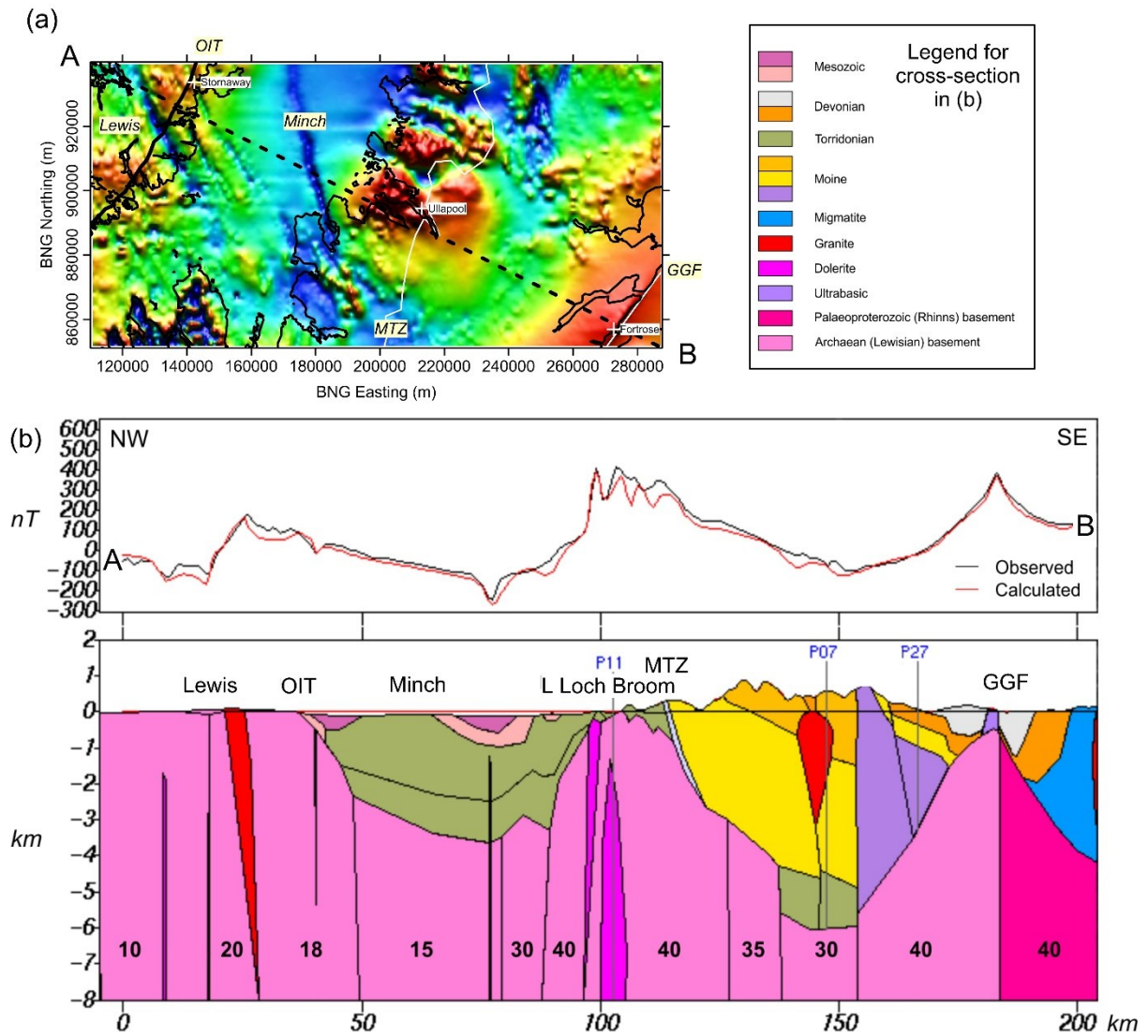


Figure 2. Hebridean study area (178 x 105 km). (a) Location map with OIT (Outer Isles Thrust, black line), Moine Thrust Zone (MTZ, white line) and Great Glen Fault (GGF, white line) identified. The coast is identified with a black line, and the main offshore area is labelled Minch. The line A-B denotes the location of the existing interpretation of magnetic structure. The background image is an equal-area histogram plot of the TMI-RTP data with a range from -1054 (blue) to 1045 nT (red). (b) Northwestern end of Profile 5 studied by Rollin (2011). The upper panel shows observed and modelled magnetic fields resulting from the model susceptibilities (values x 10⁻³ SI) shown in the lower panel. See (a) for the legend. The line A-B (0 to 200 km), from (a), is identified.

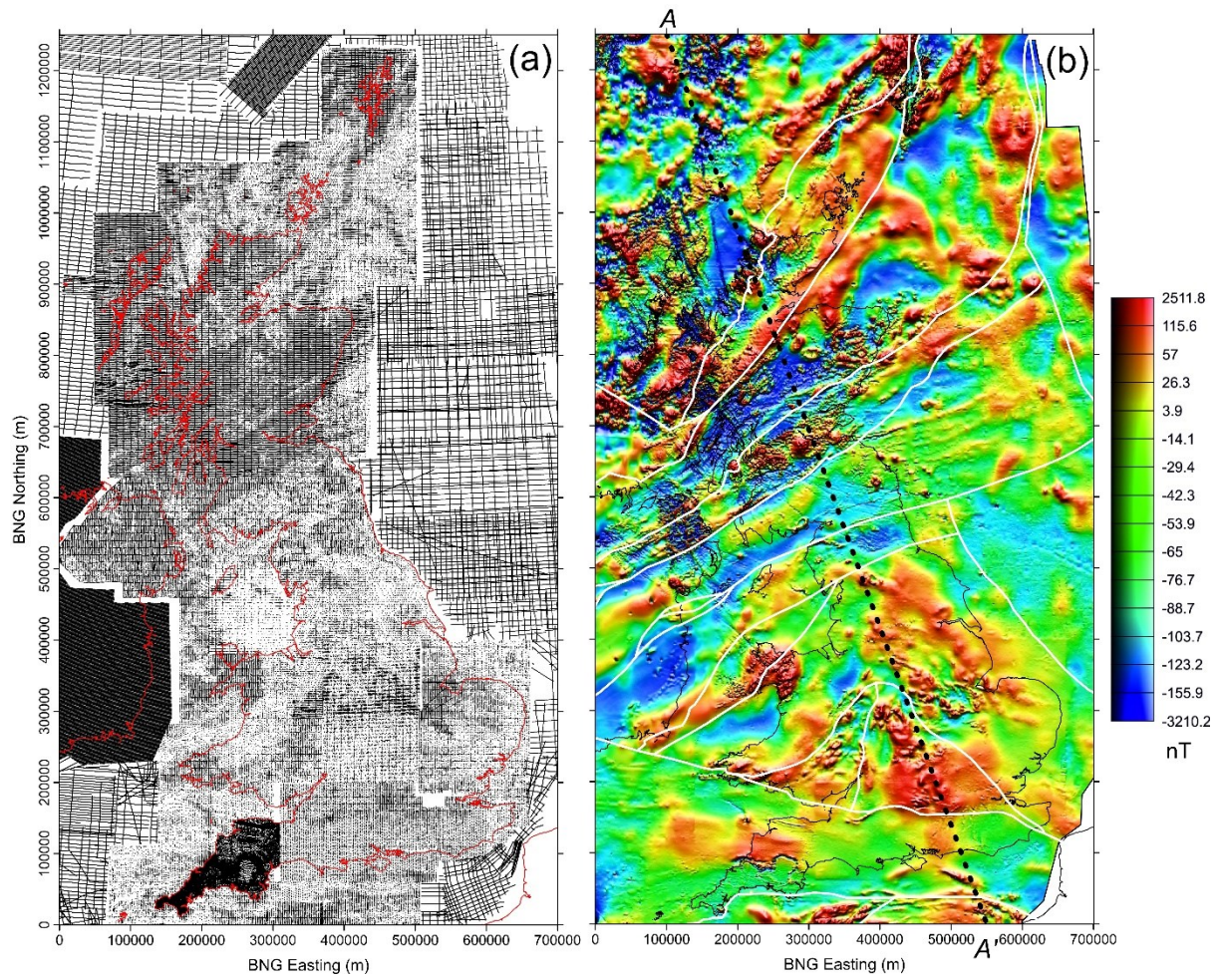


Figure 3. (a) The compiled magnetic observations (black dots) across the study area.(b) An equal-area colour image of the magnetic data compilation (reduced to pole) with terrane boundaries superimposed in white (see Fig. 1).

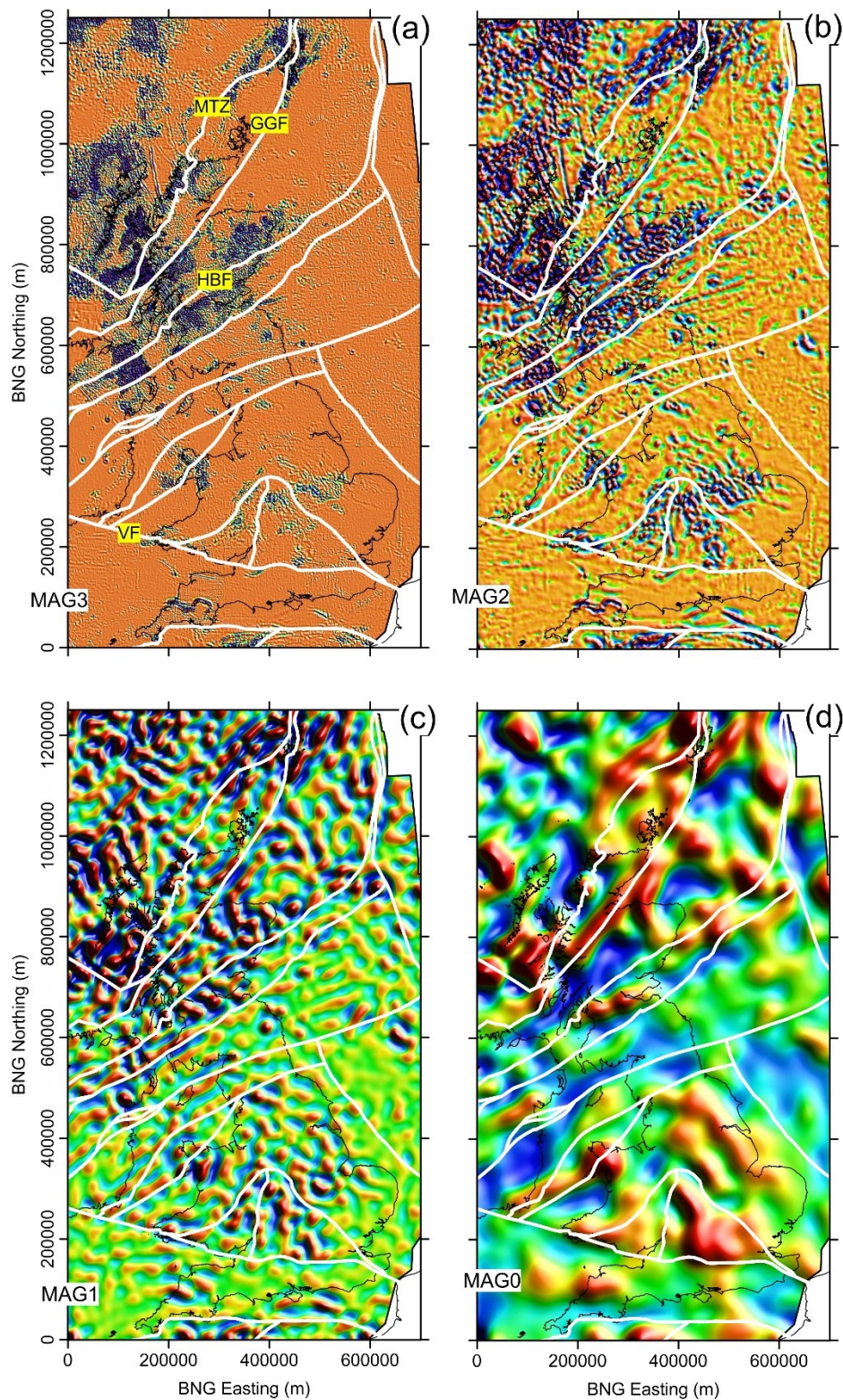


Figure 4. Equal-area colour images of the spectral decomposition of the magnetic (reduced to pole) data (see also Table 2). (a) MAG3 (spectral depth of 1609 m) with terrane boundaries superimposed in white. Four boundaries identified as MTZ (Moine Thrust Zone), GGF (Great Glen Fault), HBF (Highland Boundary Fault) and VF (Variscan Front). (b) MAG2 (spectral depth of 5018 m). (c) MAG1 (spectral depth of 16,630 m) and (d) MAG0 (spectral depth of 35,250 m). Data means and ranges of the images shown are provided in Table 2.

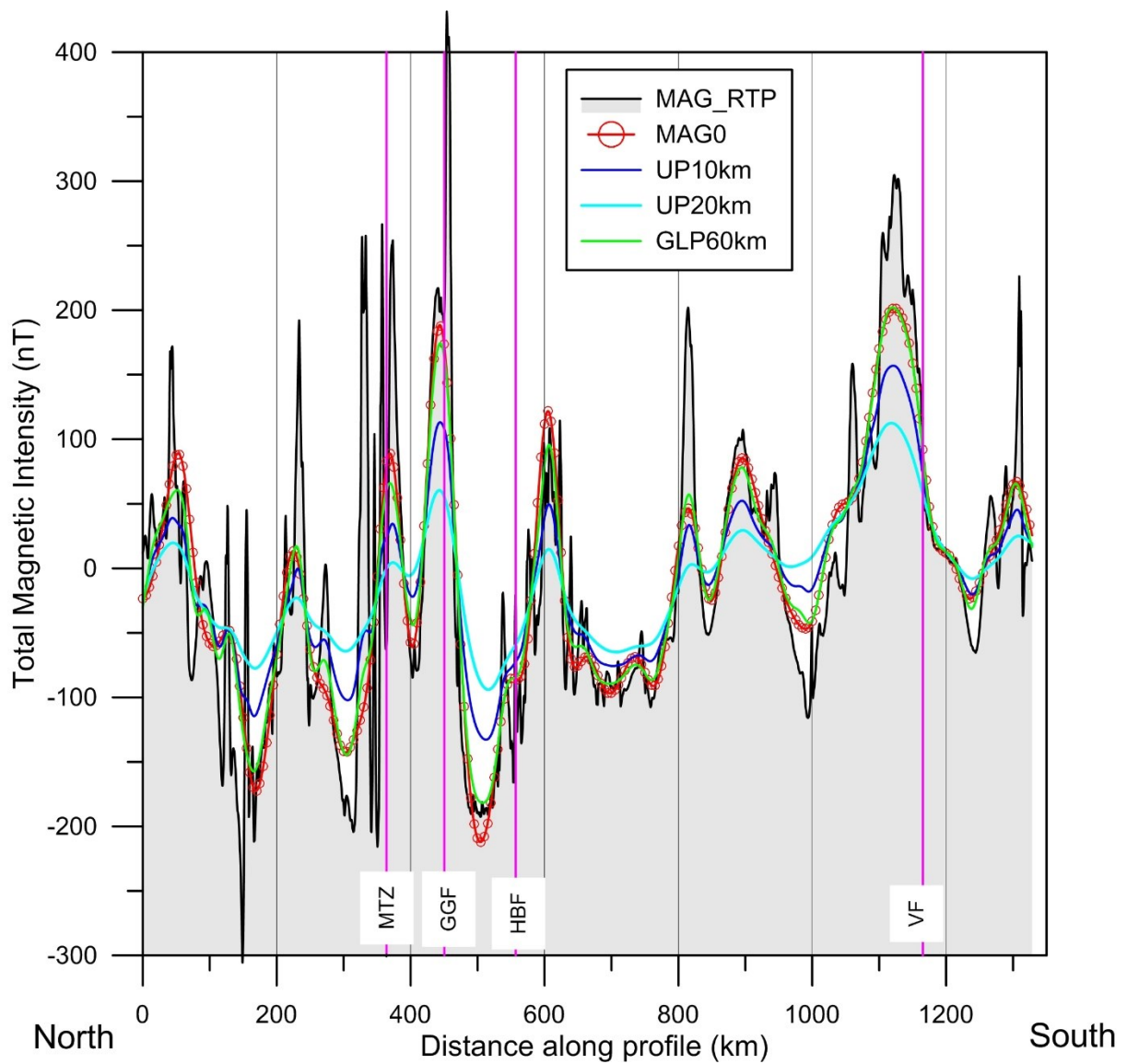


Figure 5. Comparison of TMI-RTP magnetic and filtered data along profile A-A' (see Fig. 1). Black line with grey infill shows the TMI-RTP data. Additional coloured lines (identified as MAG0, UP10km, UP20km and GLP60km) show low-pass filtered versions of the TMI-RTP data as discussed in the text. 4 terrane boundaries are identified as MTZ (Moine Thrust Zone), GGF (Great Glen Fault), HBF (Highland Boundary Fault) and VF (Variscan Front).

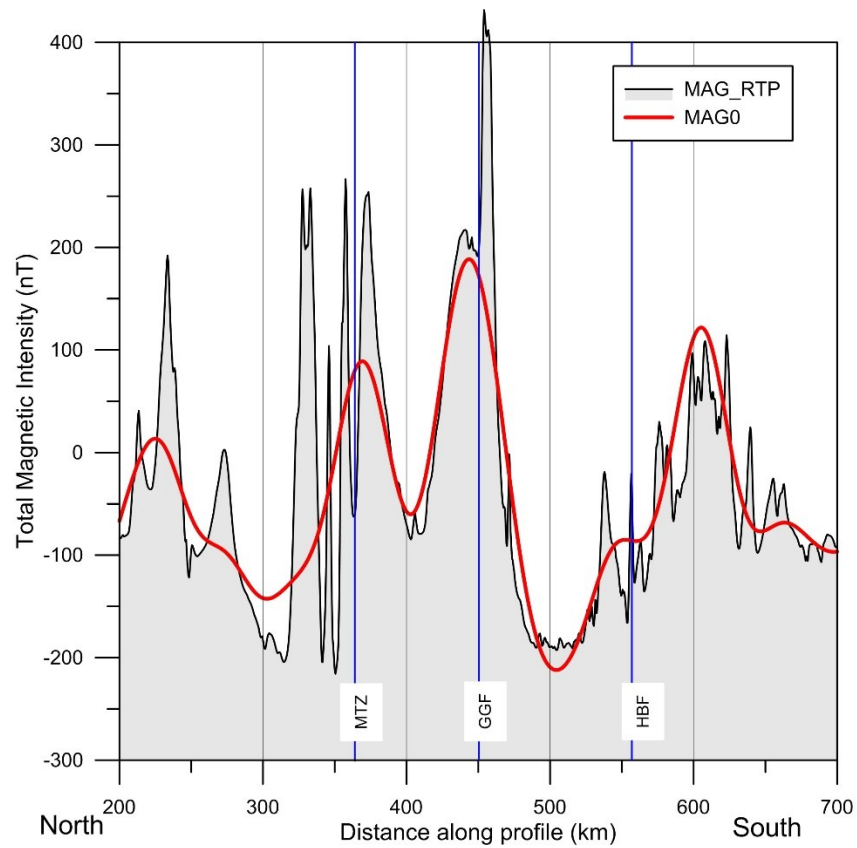


Figure 6. Detailed comparison of TMI-RTP magnetic and filtered data along part of profile A-A' (see Fig. 5). Black line with grey infill shows the TMI-RTP data. Red line shows MAG0 filtered data corresponding to the basement features. 3 terrane boundaries are identified as MTZ (Moine Thrust Zone), GGF (Great Glen Fault) and HBF (Highland Boundary Fault).

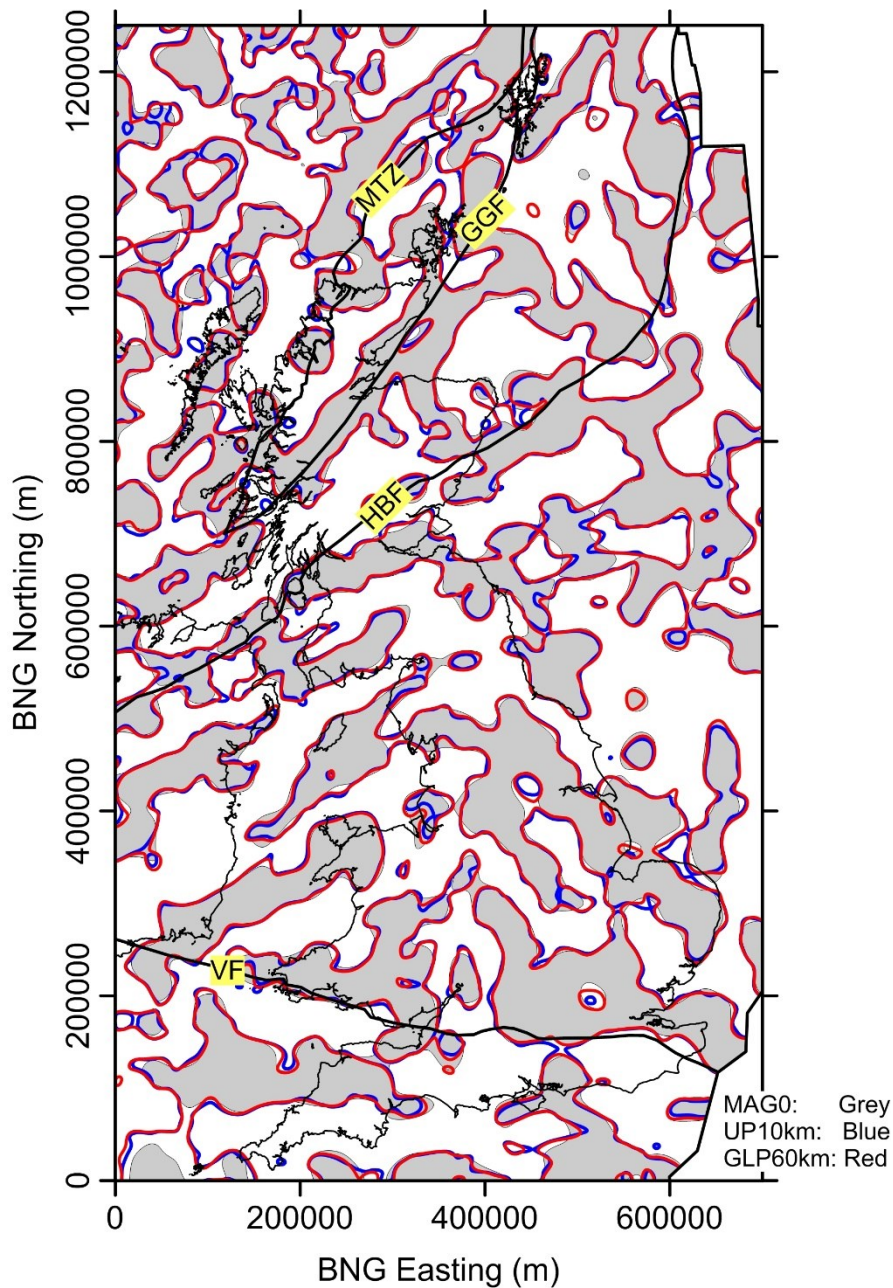


Figure 7. Comparison of tilt-derivative (TDR) zero value contours obtained by 3 low-pass filtering operations. MAG0 filtered data shown as contours with grey infill ($TDR \geq 0$). Data upward-continued by 10 km (UP10km) shown with blue contours. Gaussian regional low-pass filter (GLP60km) shown with red contours. 4 terrane boundaries are identified as MTZ (Moine Thrust Zone), GGF (Great Glen Fault), HBF (Highland Boundary Fault) and VF (Variscan Front).

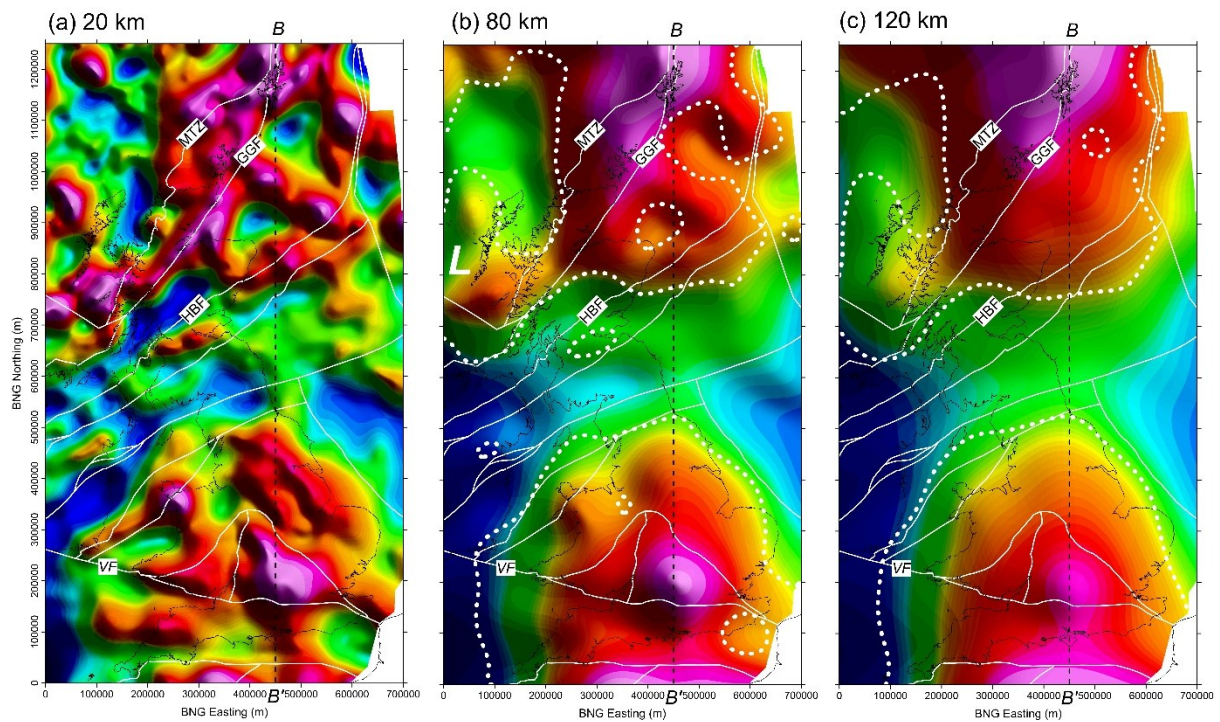


Figure 8. Comparison of 3 upward continuation levels of the TMI-RTP data. The data are shown as equal-area colour image. 4 terrane boundaries (white lines) are identified as MTZ (Moine Thrust Zone), GGF (Great Glen Fault), HBF (Highland Boundary Fault) and VF (Variscan Front). (a) Upward continuation height of 20 km. (b) Upward continuation height of 80 km with dotted line showing the contour of TDR=0 response. Letter L denotes a Limb area noted in the text. (c) Upward continuation height of 120 km with dotted line showing the contour of TDR=0 response. Amplitudes along the profile B-B' are noted in the text.

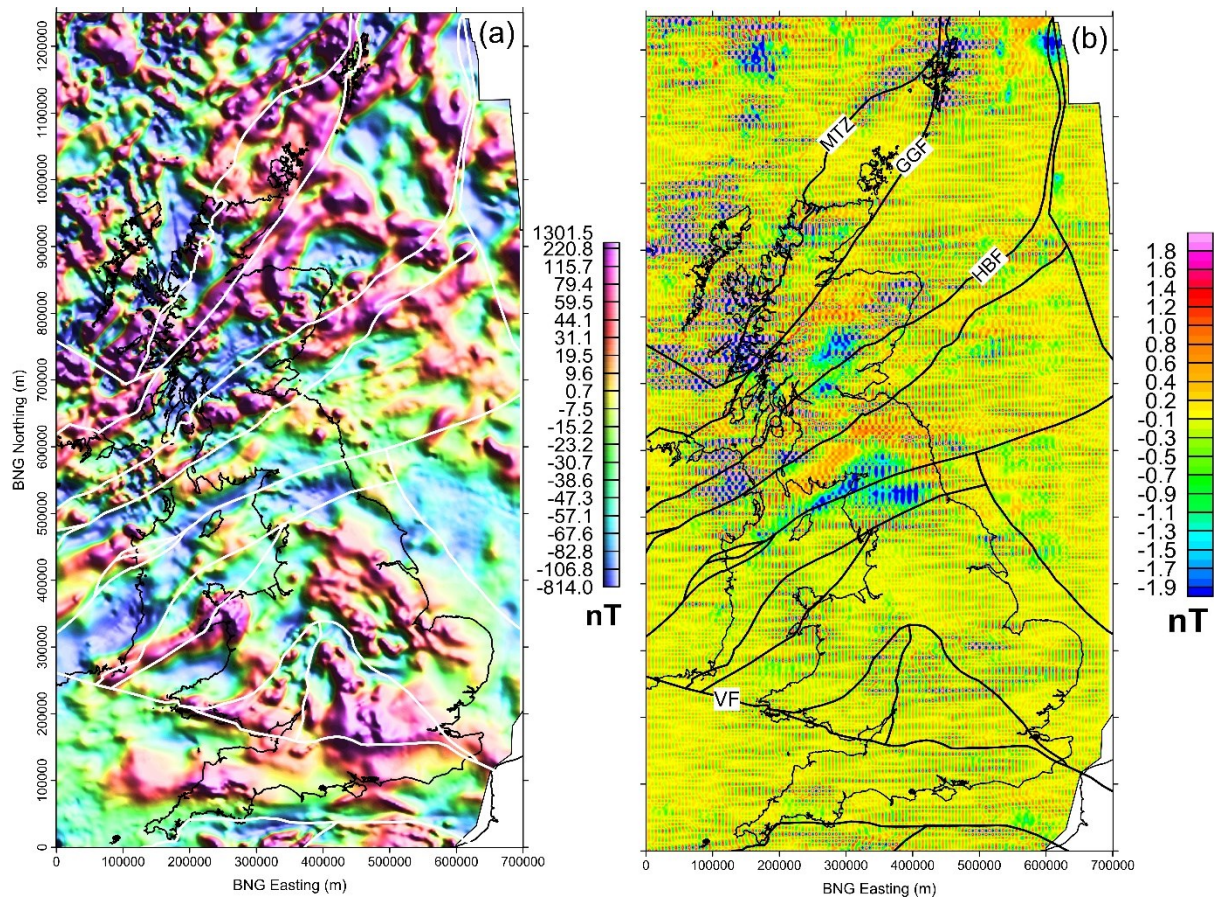


Figure 9. (a) The TMI data, gridded using a cell size of 5 km, used for 3D inversion, shown as an equal-area image with terrane boundaries (white lines) superimposed. (b) The data and modelled misfit values (observed minus modelled) shown using a linear colour scale. Terrane boundaries (black) with MTZ (Moine Thrust Zone), GGF (Great Glen Fault), HBF (Highland Boundary Fault) and VF (Variscan Front) identified.

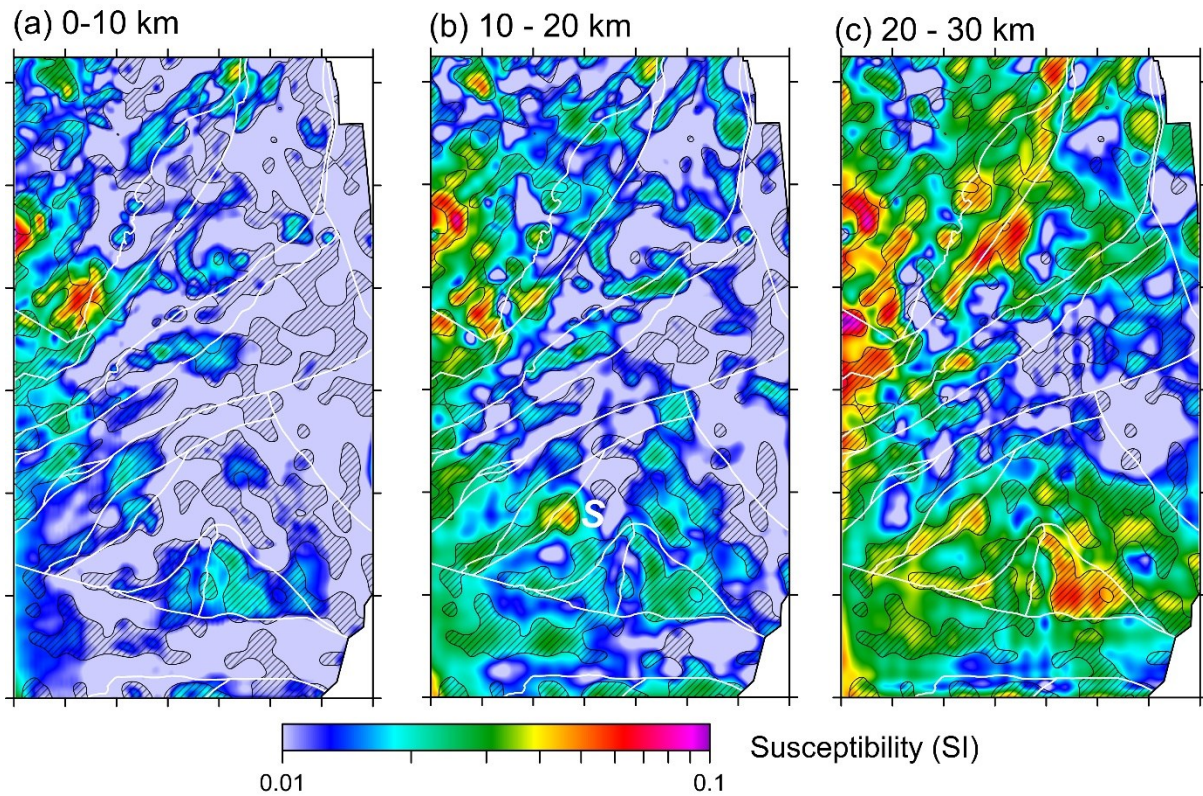


Figure 10. Three vertically integrated and normalised susceptibility depth slices summarising the 3D model results. The 3 images use the same logarithmic colour scale. (a) 0-10 km. (b) 10-20 km. (c) 20-30 km. Regions with cross-hatch denote idealised deep body source locations. S denotes Snowdon anomaly.

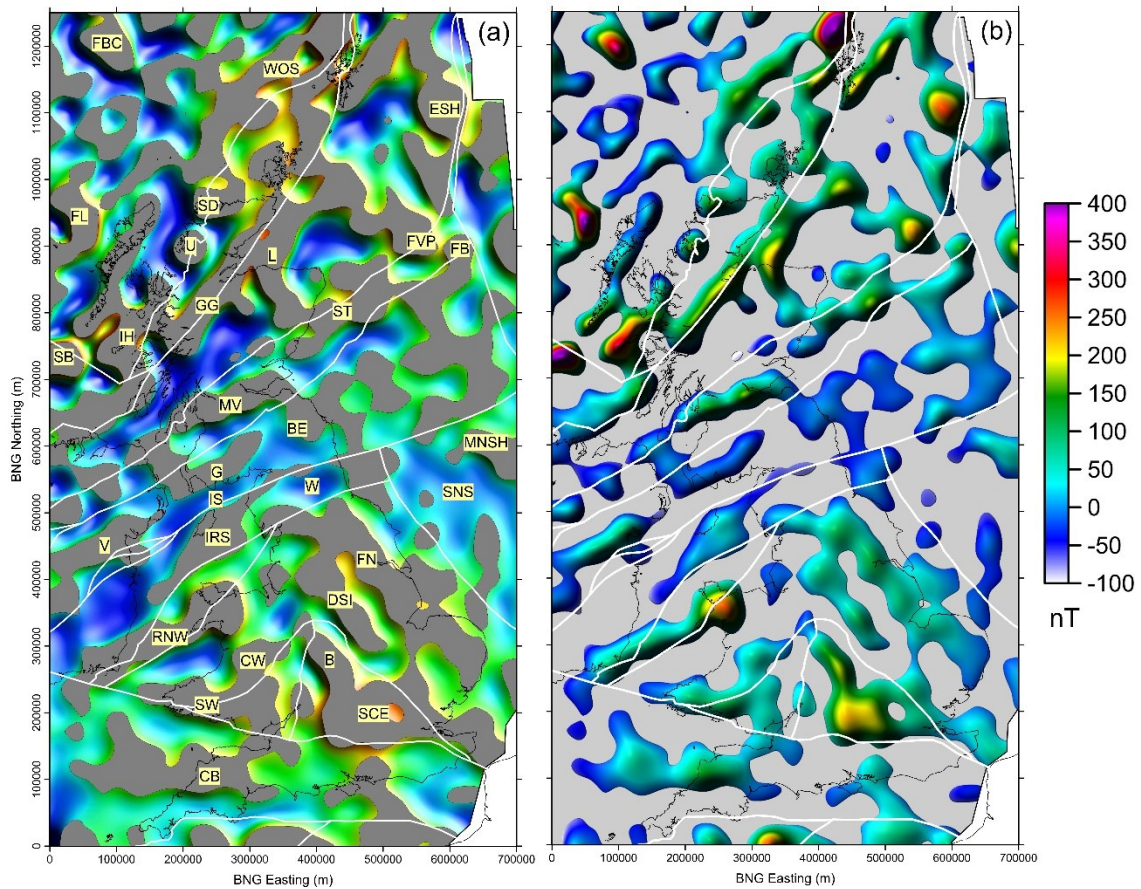


Figure 11. Tilt-derivative (TDR) analysis of the MAG0 field. (a) Contours with grey infill define $TDR \geq 0$ and outline source bodies. These contours overlay the MAG0 image shown previously in Fig. 4d. White lines denote terrane boundaries. Labels denote bodies or zones that are identified and discussed in the text (see Table 3). (b) Contours with grey infill define $TDR < 0$ and outline zones between source bodies. The colour image denotes the MAG0 magnetic field only associated with the sources (i.e. $TDR \geq 0$) and is shown using a linear colour scale.